Comparison of conventional and parameterized MPC for traffic control

A case study

Johan 't Hart

Master of Science Thesis

TU Delft Delft University of Technology

Delft Center for Systems and Control

Comparison of conventional and parameterized MPC for traffic control

A case study

Master of Science Thesis

For the degree of Master of Science in Systems and Control at Delft University of Technology

Johan 't Hart

April 05, 2011

Faculty of Mechanical, Maritime and Materials Engineering (3mE) · Delft University of Technology

Abstract

The intensity of vehicles on the road is getting higher each year resulting in an increase in the occurrence and duration of congestion. The negative impact of congestion is diverse, ranging from extra time spent in the traffic network to an increase in health problems due to the increasing emissions and fuel consumption. Dynamic traffic controllers could be used to reduce the travel time, emissions, and fuel consumption. The controller aims to steer the traffic flow so that the cost of a given objective function is minimal. This can be reached by introducing dynamic control measures, like variable speed limits and ramp metering at on-ramps. In some scenarios the reduction of travel time, emissions, and fuel consumption conflict among each other. Using the weighted-sum method, a balanced trade-off between those objectives is obtained.

The dynamic traffic control approach considered in this research is Model Predictive Control (MPC). Via a prediction of the traffic states, the controller optimizes the sequence of the control inputs over a prediction horizon to minimize the criteria in the cost function. The optimal control inputs are translated on-line to the variable speed limits and ramp metering rates. The next control time step the optimization is carried out again using new obtained data, to find the new optimal control inputs. MPC computes the optimal control inputs based on a model of the traffic flow and a model of the emissions and fuel consumption rates. The METANET model is chosen to compute the traffic flow, whereas the VT-macro model is chosen to compute the emissions and fuel consumption.

One of the major disadvantages of conventional MPC is the large computation time required to solve the optimization problem. To reduce the computational complexity of the optimization problem, an alternative approach, parameterized MPC, is considered. In this approach the control inputs are computed according to some control laws, that relate the control inputs to the traffic states and traffic outputs. The optimization algorithm has to optimize the parameters used in the control laws to find the optimal control inputs. This will significantly reduce the computational complexity of the optimization problem and could make the controller fast enough for on-line control of the freeway. The main question is how to define the control laws, so that the controller is still able to compute the optimal control inputs and in the meantime reduce the computation time.

The approach described above is applied to a case study of a part of the Dutch A12 free-

way, between Bodegraven and Woerden Oost. For a given demand profile, the conventional MPC requires 9-10 hours to simulate a freeway of 14 km for a simulation period of 1 hour. For different weights of the criteria, the controller is able to reduce 20% of the travel time, and 40% of the total emissions and fuel consumption. Practically the same performance can be obtained for parameterized MPC, however, in a timespan of 1 - 35 minutes for different sets of control laws. This thesis has therefore concluded that, based on the outcome of the scenario, the parameterized MPC approach is a good alternative for conventional MPC for the use of on-line dynamic traffic control.

Table of Contents

Preface

During the last year I have been practicing my knowledge obtained in the master Systems and Control on a case study resembling a part of the Dutch A12 freeway. I have had the opportunity to use the theory to tackle a relevant problem of the society.

The topic of my research is to develop a controller that can be used to on-line control the traffic flow on a freeway. There are two reasons why I choose this topic. On the one hand, I liked to be able to apply my knowledge to real life problems and in the meantime explore the effect of my research. What can I do with my knowledge? How does it affect, in this case, the traffic flow? On the other hand, this project gave me the opportunity to focus on sustainability issues as well. The focus of the controller is not only to improve the travel time of vehicles on a freeway, but also to reduce the emissions and fuel consumption of vehicles. In this way, I could combine my Bachelor study (Sustainable Molecular Science and Technology) with the Master System and Control. A major part of the Bachelor was on sustainable development.

This project is conducted in several phases. In the first phase I have been looking at the models that are used in the control approach. The next phase was to model the traffic flow and compute the optimal control input to minimize the travel time, emissions, and fuel consumption. The final phase was to collect and analyze the obtained results. This report is the result of these phases.

I could not have done this all by myself. I would like to thank Solomon Zegeye, MSc for his coaching. Solomon was my direct supervisor in this project. He provided me with the first set of papers to conduct my literature research, and with the model for MPC to start the thesis project. During the project I could always ask questions and get feedback from him.

Secondly, I like to thank prof. dr. ir. B. De Schutter for supervising me. During our monthly meetings I always got feedback so that I could continue when I found myself stuck somewhere.

Next to my supervisors, I also like to mention my fellow students, my family, and my friends who have been there for me, making this project bearable. Finally, I want to thank the Lord for giving me the wisdom to complete this thesis project.

Sincerely,
Johan 't Hart

Chapter 1

Introduction

1-1 Impact of congestion

Freeways all over the world have to deal with increasing numbers of vehicles on the road, resulting in flows that exceed the capacity of the freeways. This phenomenon has led to an increase in the occurrence and duration of congestion [6], [22]. All over the world, measures are taken to reduce congestion, such as speed limits, provision of congestion information, or on-ramp metering. Several studies have shown that traffic jams and traffic breakdowns have a negative impact on the drivers themselves, the environment, and the society as a whole [2], [32], [36], [45]. First of all, the mobility of vehicles in and around cities is largely reduced by traffic jams. Furthermore, the higher intensities of vehicles on the road cause an increase in the emissions and fuel consumption rates, a decrease of the safety and quality of life, and an increase of the economical costs. These points are elaborated next.

- *Travel time.* Traffic jams increase the travel time of vehicles, as vehicles cannot drive at the maximal allowed speed. Furthermore, congestion on freeways could spill back to local roads around cities, affecting the travel time of other vehicles as well [21].
- *Safety.* The chance of accidents in dense traffic flows is higher than in sparse traffic flows, since in dense traffic flows drivers react more heavily to changes in the relative speed between their vehicle and the leading vehicle. Often, this results in an unstable situation where a minor disturbance could have a major impact.
- *Quality of life.* Drivers, passengers, and people living nearby major freeways will encounter increasing health problems, like bronchitis, asthma, reduced lung function, or even mortality, due to the high level of emissions they are exposed to. In some scenarios congestion results in concentration of emissions that exceed the safety levels (e.g., nitrogen dioxide and particulates) [5], [36]. Furthermore, the increase in emissions (like CO_2) and fuel consumption due to congestion also contributes to the global climate change worldwide [36]. Congestion also reduces the comfortability of drivers, as they

have to spend longer time in the vehicles. They are then easily stressed and frustrated as they have to endure (large) delays. More vehicles on the road also lead to higher noise productions. This affects the drivers themselves, but also the people living in the neighborhood of the traffic network. Another effect of the occurrence of congestion is the fact that drivers should leave earlier from home and later from work to avoid congestion.

- *Economical issues.* The increasing travel time and fuel consumption also affect the economy. On the one hand longer unproductive hours are spent in the traffic networks, on the other hand a larger amount of fuel is consumed due to the traffic jams. As the price of fuel increases, the costs of traffic jams also increase. The impact of traffic jams and delays on the economy is estimated at 2.7 - 3.6 billion euro for the traffic network in The Netherlands in 2008 [54].

1-2 Dynamic traffic management

1-2-1 Motivation

In the last decades the intensity of vehicles on freeways in The Netherlands has grown [9]. The current capacity on freeways is not always able to handle this demand resulting in frequent traffic breakdowns and traffic jams. In order to tackle this increasing problem the operational capacity on freeways should be increased. There are multiple solutions that can be explored that could increase the operational capacity on freeways, such as the construction of new roads, the use of intelligent vehicles, or the use of dynamic traffic management [10]. On the short term, dynamic traffic management seems to be a sound solution. Most of the necessary installations are already available on freeways or can easily be installed. It requires, e.g., message signs above freeways, loop detectors in the roads, ramp metering installations at on-ramps, or traffic signal systems at intersections of freeways.

According to [42] the operational capacity on freeways is underutilized. In other words, with some intelligent control the capacity efficiency on freeways can be increased, without the construction of new roads. By applying dynamic control inputs the throughput of the traffic flow can be improved and congestion reduced. Various control inputs could be considered to achieve this goal among which are variable speed limits, ramp metering rates, and route guidance [32]. Variable speed limits can be used to control the density of the vehicles on freeways. By regulating the maximum speed the traffic flow can be smoothened. For instance, if a high density wave downstream a freeway is higher than the critical density, a low density wave can be formed upstream by the actuated speed limits to compensate for the high density wave. This will counteract the formation of shock waves [23]. Ramp metering rates can regulate the inflow of the vehicles from the on-ramp to the freeway [42]. A lot of congestion occurs in the vicinity of on-ramps due to the merging behavior of vehicles that want to enter the freeway. By limiting this number, the merging behavior can be controlled and thereby congestion is reduced. Route guidance could also limit the number of vehicles that want to enter the freeway by rerouting vehicles to other roads. By rerouting vehicles, the intensity of vehicles on the available roads is spread more equally, which could prevent congestion [40]. The study performed in this thesis is restricted to the use of variable speed limits and ramp

metering rates, because route guidance requires a more complex model of the traffic flow [33], which is beyond the scope of the thesis project.

The values of the optimal control inputs (variable speed limits and ramp metering rates) that steer the traffic flow in the desired direction depend on the goal of the controller. Such goal could be to reduce the travel time, to maintain a certain level of safety, or to reduce the emissions or fuel consumption. These criteria sometimes coincide, and sometimes conflict with each other. For example, the emissions of vehicles are higher when they drive at the maximum allowed speed than for lower speeds, but the travel time is lower for higher speeds [12]. When the focus of the controller lies only on the reduction of emissions, this could lead to other values of the optimal control input than when the focus would lie on the reduction of the travel time. Therefore, it could be wise to combine the criteria to get a balanced trade-off between those criteria. The focus of the controller in this project is chosen to be a combination of the reduction of the travel time, emissions, and fuel consumption.

1-2-2 Model predictive control approach

Now that the control measures are selected, the question remains how the optimal values for these control measures can be computed, so that the goal of the controller is met. In the literature many approaches are suggested to compute these values (e.g., [10], [26], [35], or [42]). One of the approaches discussed is Model Predictive Control (MPC) [22]. Using traffic models that represent the real traffic behavior, emissions rates, and fuel consumption rates MPC estimates and predicts the current and future traffic states from measurement data and a priori knowledge. Via an optimization algorithm the MPC controller computes the optimal control inputs over the predicted horizon that minimizes an user-defined cost function under certain conditions (e.g., from now to 15 min in the future). Next, it applies the control inputs corresponding to the next time step to the real traffic system. Finally, in the first time step some new measurement data is available from the real traffic flow and the procedure can be started all over again using a shifted prediction horizon.

MPC has several advantages that makes it very suitable for on-line dynamic traffic control [7], [8]. First of all, MPC can be applied to nonlinear time-varying models, as in fact the traffic flow is. Secondly, it can handle (nonlinear) constraints (e.g., maximum queue lengths at on-ramps), multi-criteria cost functions, and disturbances or model uncertainties. Thirdly, MPC is very flexible in the sense that it can be easily adapted to other traffic situations [22]. For instance, when a lane on a part of the freeway is closed due to work or an incident, it can be adapted on-line in the model.

The major drawback of MPC is the required computation time. Although it is in many cases faster than conventional optimal control approaches it still is too slow for on-line control [22], [58]. One of the goals in this thesis is therefore to find a way to reduce this computation time without compromising the advantages of MPC listed above and without loosing accuracy. The required computation time is large due to the fact that the controller needs to find the optimal values for all control inputs over a the prediction period. In order to speed up this process the control inputs could be computed indirectly using control laws. These control laws relate the control inputs (variable speed limits and ramp metering rates) to the traffic states and outputs (e.g., density, speed). The optimization algorithm then only has to optimize the parameters used in the control laws to find the optimal control inputs. When the control laws are defined such that the number of parameters is less than the number of control inputs, the

required computation time could be reduced as the optimization algorithm has to optimize less parameters. The use of control laws to compute the control inputs is called parameterized Model Predictive Control [1], [58].

1-3 Problem statement

1-3-1 Research questions

The goal of the thesis is to develop a dynamic traffic controller that is able to, on the one hand, minimize the travel time, emissions, and fuel consumption of vehicles on freeways and, on the other hand, compute the optimal control sequence fast enough for on-line control. The approach studied in this thesis is the Model Predictive Control approach.

In order to achieve this goal, the following research questions are formulated:

1. Are the models used in the MPC approach a good representation of the real traffic behavior?
2. What are the available dynamic traffic control measures that could be used to steer the traffic flow?
3. How does the control approach deal with a multi-criteria control objective (travel time, emissions, and fuel consumption) in the computation of the optimal control inputs?
4. Is the developed controller able to compute the optimal control inputs within a given time frame? If not, how can the controller be altered so that the required computation time is less than the given time frame?
5. Is the parameterized MPC approach able to maintain a similar level of accuracy compared to conventional MPC, while reducing the required computation time?

1-3-2 Methodology

In order to answer the research questions, first a literature survey is conducted to determine which models accurately represent the traffic behavior and can be applied in the MPC framework. Once the models are selected, they are implemented in MATLAB®, to simulate the traffic behavior. Next, the objective of the control approach is defined, in the form of a cost function. Two different methods to define this cost function are studied, one of which is selected next for further use in the project.

To test the MPC control approach a case study is conducted. Real data and the real network lay-out involving part of the Dutch A12 freeway, between Bodegraven and Woerden, are used to simulate the traffic behavior for a given demand profile. The chosen demand profile results in congestion when no control is active. In this way, it can be seen whether or not MPC is able to resolve the congestion. The control approach is set under certain constraints that are also active in the real traffic network. Additional constraints, like maximum queue lengths at on-ramps, are implemented to see how MPC deals with these constraints and how the control inputs are effected by these constraints. The dynamic traffic control measures to

control the traffic flow are chosen to be the variable speed limits and the ramp metering rates.

To parameterize the conventional MPC approach, some control laws are defined. These control laws are implemented in the MPC framework and tested under the same conditions as the conventional MPC approach. The required computation time is recorded and the accuracy of the parameterized MPC controller is compared to the conventional MPC controller. From these results a conclusion is drawn towards the use of parameterized MPC in general and the control laws studied in particular, for applications of on-line dynamic traffic control.

1-4 Outline of the chapters

The structure of the report is as follows. In Chapter 2 the traffic models used in the MPC approach are explained. The chapter presents an overview of the available models that describe the traffic behavior and gives the equations of the METANET and VT-Macro models. Chapter 3 discusses the concept of the conventional MPC approach. Chapter 4 presents the parameterized MPC approach. It states the motivation for the parameterization and provides the general framework for parameterization of the control inputs.

Chapter 5 describes the case study in detail and explains the set-up for the scenarios studied in this thesis. It presents the results for conventional and parameterized MPC and makes a comparison between these methods.

Finally, Chapter 6 provides the conclusions and outlines future work. The chapter summarizes the answers to the research questions and gives some suggestions and recommendations for further research.

Chapter 2

Traffic models

The dynamic traffic control approach MPC is a model-based approach. Using measurement data and a priori knowledge as input, the model estimates and predicts the current and future traffic behavior. Based on this prediction the MPC approach computes the optimal control inputs to steer the traffic flow in the desired direction. It is therefore important that the model used in the MPC approach accurately and efficiently represents the real behavior of traffic flow, emissions and fuel consumption.

Prior to this thesis a literature survey has been conducted to select the most suitable model for this approach. From this survey it became clear that there are two models required to represent the traffic behavior. One model to describe the traffic flow and one to compute the traffic emissions and fuel consumption of the traffic flow.

In Section 2-1 an overview of traffic flow models will be discussed, from which METANET is chosen to be used in the MPC approach. In Section 2-2 the traffic emissions and fuel consumption models are discussed, from which VT-Macro will be selected. Note, however, that MPC is a general approach that can use other models as well. So, when a model that is more accurate or that requires less computation time is available, this model can easily be implemented in MPC too.

2-1 Traffic flow models

2-1-1 Overview of traffic flow models

Microscopic and macroscopic traffic flow models

Traffic flow models can be classified as either microscopic traffic flow models or macroscopic traffic flow models [25]. The former ones describe the behavior of individual vehicles with respect to their direct surroundings. The latter ones describe the behavior of vehicles as a continuous stream, more on an aggregate level. Some traffic flow models are in between those classes and are called mesoscopic traffic flow models.

Microscopic models are often based on car-following behavior and lane-change behavior

[25], [30]. A car-following model describes the distance between two consecutive vehicles. It describes the reaction of the follower when the leader is changing its speed. A lane-change model describes the possibility of the follower to overtake the leader. It computes this overtake manoeuvre based on the available gap, the speed difference with its predecessor, the attitude of the driver and so on. Using these two models microscopic traffic flow models estimate the behavior of all individual vehicles which together leads to one model of the traffic flow.

Macroscopic traffic flow models, on the contrary, describe the aggregate behavior of vehicles [30]. They compare the stream of vehicles with a stream of fluid flowing through a pipe. Using the conservation law of mass, they make a balance of vehicles: the number of vehicles in the network is equal to the number of vehicles entering the network minus the number of vehicles leaving the network plus the number of vehicles that stays in the network. They (sometimes) also use additional equations, e.g., speed equation. Macroscopic models are therefore based on the average speed of vehicles and the intensity of vehicles on the road (density).

Microscopic traffic flow models can describe the traffic flow very accurately as they incorporate every movement of all the vehicles in one model. However, microscopic traffic flow models depend on a lot of parameters, such as the attitude of the drivers, the acceleration of vehicles, the type of road or weather conditions, which makes them hard to calibrate in order to represent the real traffic flow, using the limited amount of data available. Another drawback is the fact that microscopic traffic flow models have to compute the behavior of all individual vehicles. The more vehicles on the road, the larger the computation time will be, as for each vehicle a number of equations has to be solved. For large-scale traffic networks, such as freeways, microscopic traffic flow models are not suitable for on-line applications [25].

Macroscopic traffic flow models are often less accurate than microscopic traffic flow models, as they model only the aggregate behavior of vehicles and not the individual behavior. However, this largely reduces the number of parameters that have to be calibrated. In fact, with the available data set obtained from loop detectors in the road, the model can easily be calibrated [32]. Also, the complexity of the model does not depend on the number of vehicles in the network. As macroscopic traffic flow models only use aggregate states of the vehicles, the number of equations to be solved remains the same for every amount of vehicles in the traffic network and as a result they are much less computationally intensive than microscopic traffic models.

The control inputs used to control the traffic flow, such as variable speed limits and ramp metering rates, aim to steer the aggregate behavior of vehicles rather than the individual behavior of vehicles. Therefore, for these control purposes the use of macroscopic traffic flow models is accurate enough to represent the traffic flow behavior. Given the advantages of macroscopic traffic flow models with respect to microscopic traffic flow models, the model used in the MPC approach is preferred to be macroscopic [25].

Types of macroscopic traffic flow models

There are three main types of macroscopic traffic flow models, based on the order of the model. All of these types are founded on the conservation of vehicles. The first type of macroscopic traffic flow models was developed by Lighthill, Whitham, and Richards in 1955 and 1956 and is known as LWR-type models [37]. This model assumes that the density on the road can describe the desired speed of vehicles. Using this relation a first-order partial differential equation can be formulated. The main drawback of this type of macroscopic traffic

flow model is the fact that the equations do not yield a unique solution. Therefore, this model uses characteristic curves to determine the flow [25].

In 1971 Payne developed a second-order macroscopic traffic flow model, known as Payne-type model [44]. His model is based on two partial differential equations. He extended the LWR-type model by incorporating the relationship between the actual speed and the desired speed of vehicles, based on the car-following model. He identified in his expression a convection, relaxation, and anticipation term.

The third-order macroscopic traffic flow model was developed in 1996 by Helbing [24]. He describes the behavior of traffic based on three partial differential equations, by taking the density, speed, and the variance of the speed as states.

The type of macroscopic model chosen for this case study is the Payne-type model. The LWR-type models are too simplistic to describe the traffic flow in an accurate way [25]. The Helbing-type models are too complex. It has been shown in the literature that second-order type models are able to describe the traffic flow in an accurate way [32], [42]. METANET [39] is one of the most frequently used second-order macroscopic traffic flow models and will be used in this case study as well.

2-1-2 Extended METANET model

The traffic flow model selected for this case study is an extended version of the model METANET [39], which is a second-order macroscopic traffic flow model. METANET has the ability to model the traffic flow accurate enough for control purposes, while the computational complexity of the model is far less than for microscopic traffic flow models. Besides the complexity, the model has also the advantage that it can be easily calibrated with data generated by loop detectors in the road. The model can be applied to free-flow, dense, or congested traffic conditions with prescribed characteristics (location, intensity, duration). Furthermore, METANET can be used in combination with dynamic control inputs, such as ramp metering rates and variable speed limits.

Model description

METANET is based on Payne's model, but it uses discrete states instead of continuous ones. The discretization is done both in time and space. The time discretization step is global and defined as T_s, but the space discretization strip is defined differently. The traffic network is represented by links and nodes, whereby links represent homogeneous freeway stretches. Each freeway stretch has uniform characteristics, such as the same number of lanes along the freeway stretch or the same road geometry. A node is placed at locations where a major change in the road geometry occurs, as well as at junctions, on-ramps, and off-ramps.

A freeway link is divided into N_m segments of length L_m. For each segment i of each link m at each time step $t = k \cdot T_s$ for $k = 0, 1, \cdots$ the macroscopic variables flow, density, and space-mean speed are computed. Figures 2-1(a) and 2-1(b) illustrate the discretization of a freeway network into links and nodes, and the discretization of links into segments, respectively.

Freeway network links

The METANET model consists of freeway links, origin links, and destination links. Each of these links has its own set of equations.

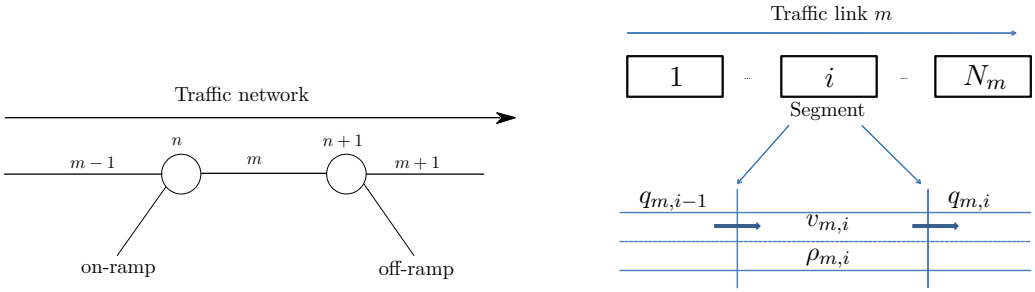

(a) Traffic network (b) Traffic link

Figure 2-1: Traffic network discretized into links m and nodes n (a). Links are further discretized into segments (b)

Freeway links are described by the equations of the Payne model [44], but then discretized in time and space.

$$q_{m,i}(k) = \rho_{m,i}(k) v_{m,i}(k) \lambda_m \tag{2-1}$$

$$\rho_{m,i}(k+1) = \rho_{m,i}(k) + \frac{T_s}{L_m \lambda_m} \left(q_{m,i-1}(k) - q_{m,i}(k) \right) \tag{2-2}$$

$$\begin{aligned} v_{m,i}(k+1) = v_{m,i}(k) &+ \frac{T_s}{\tau} (V[\rho_{m,i}(k)] - v_{m,i}(k)) + \frac{T_s}{L_m} v_{m,i}(k) \left(v_{m,i-1}(k) - v_{m,i}(k) \right) \\ &- \frac{\nu T_s}{\tau L_m} \frac{\rho_{m,i+1}(k) - \rho_{m,i}(k)}{\rho_{m,i}(k) + \kappa} \end{aligned} \tag{2-3}$$

where $q_{m,i}(k)$, $\rho_{m,i}(k)$, and $v_{m,i}(k)$ are the flow, density, and space-mean speed of link m of segment i at time step k, λ_m denotes the number of lanes of link m, L_m denotes the length of the segments of link m, and $V[\rho_{m,i}(k)]$ denotes the desired or equilibrium speed of the vehicles as a function of the density of link m of segment i. The parameter τ is a time constant, the parameter ν is an anticipation constant, and the parameter κ is a model parameter.

The equilibrium speed $V[\rho_{m,i}(k)]$ is empirically determined and takes the form

$$V[\rho_{m,i}(k)] = v_{\text{free},m} \exp \left[-\frac{1}{a_m} \left(\frac{\rho_{m,i}(k)}{\rho_{\text{crit},m}} \right)^{a_m} \right] \tag{2-4}$$

where $v_{\text{free},m}$ denotes the free-flow speed of link m and $\rho_{\text{crit},m}$ the critical density per lane of link m. The variable a_m is a parameter of the fundamental diagram.

In order to account for the speed reduction caused by merging phenomena in the vicinity of an on-ramp, the term

$$-\frac{\delta T_s q_o(k) v_{m,1}(k)}{L_m \lambda_m (\rho_{m,1}(k) + \kappa)} \tag{2-5}$$

is added to Equation 2-3, where δ is a model parameter and $q_o(k)$ is the inflow into the traffic network from origin o at time step k.

In order to account for the speed reduction caused by weaving phenomena when there is a lane drop the term

$$-\frac{\psi T_s \Delta \lambda_m \rho_{m,N_m}(k) v^2_{m,N_m}(k)}{L_m \lambda_m \rho_{\text{crit},m}} \tag{2-6}$$

is added to Equation 2-3, where ψ is a model parameter and $\Delta\lambda_m$ is the difference in lanes at that location.

Origin links are placed at the origins of the network, such as on-ramps or mainstream origins. They can be described by a simple queue model, where it is assumed that the inflow of vehicles to the network is not dependent of the traffic conditions downstream of the freeway. The equation is given by

$$w_o(k+1) = w_o(k) + T_\mathrm{s}(d_o(k) - q_o(k)) \tag{2-7}$$

where $w_o(k)$ denotes the queue length at the origin o at time step k, $d_o(k)$ denotes the demand of the origin o at time step k, and $q_o(k)$ denotes the outflow of the origin o into the traffic network at time step k. The outflow is dependent on the demand of the origin, the traffic conditions of the first segment of the entering link, and the ramp metering rate applied at the origin

$$q_o(k) = \min\left[d_o(k) + \frac{w_o(k)}{T_\mathrm{s}}, Q_o \cdot r_o(k), Q_o\left(\frac{\rho_{\max,m} - \rho_{m,1}(k)}{\rho_{\max,m} - \rho_{\mathrm{crit},m}}\right)\right] \tag{2-8}$$

where the variable $Q_o(k)$ is the capacity of the road of the origin o at time step k and $\rho_{\max,m}$ and $\rho_{\mathrm{crit},m}$ are the maximum and critical density of link m connected to origin o, respectively. The variable $r_o(k)$ is the ramp metering rate of origin o at time step k and lies in the range $[r_\mathrm{min}, 1]$, where r_min is the minimum allowed rate at that origin. This allows the model to control the input to the freeway network.

Destination links are bounded by the downstream traffic conditions. If no measurements for boundary conditions are available, it is assumed that the downstream traffic conditions are not congested

$$\rho_{m,N_m+1}(k) < \rho_{\mathrm{crit},m} \tag{2-9}$$

$$v_{m,N_m+1}(k) = v_{\mathrm{free},m} \tag{2-10}$$

where $\rho_{m,N_m+1}(k)$ and $v_{m,N_m+1}(k)$ are respectively the virtual density and speed of link m connected to a destination (end of considered traffic network or an off-ramp).

Freeway network nodes

Freeway network nodes are placed to connect the links to each other. The nodes of the network are modeled without any dynamic behavior. The nodes distribute the traffic flow that enters the node n via the links μ upstream the node to the exiting links σ downstream the node. The turning rate $\beta_{\sigma,n}(k)$ is introduced to decide the ratio of vehicles that leaves the node n to a specific exiting link σ. E.g., when the traffic network has an off-ramp, the node splits the traffic flow into two parts, where one part remains on the freeway, while the other part leaves the traffic network via the off-ramp. Also, when an on-ramp is present, the node combines the flow of the freeway with the flow of the on-ramp into one flow, downstream the on-ramp. The equation to describe this behavior is given by

$$\begin{aligned} Q_n(k) &= \sum_{\mu\in\mathcal{I}_n} q_{\mu,N_\mu}(k) && \forall n \\ q_{\sigma,0}(k) &= \beta_{\sigma,n}(k)\cdot Q_n(k) && \forall \sigma \in \mathcal{O}_n \end{aligned} \tag{2-11}$$

where $Q_n(k)$ is the total traffic flow entering node n at time step k, $\mathcal{I}_n$ is the set of links entering node n, and $\mathcal{O}_n$ is the set of links leaving node n.

When a node has more than one leaving links (e.g., at off-ramps), the density on both these links has to be taken into account to compute the speed of the last segment N_μ of link μ entering the node in Equation 2-3. This speed is affected by the downstream density (anticipation term of the equation). To incorporate both densities, a so-called virtual downstream density is defined as

$$\rho_{\mu,N_\mu+1}(k) = \frac{\sum_{\sigma\in\mathcal{O}_n} \rho_{\sigma,1}^2(k)}{\sum_{\sigma\in\mathcal{O}_n} \rho_{\sigma,1}(k)} \tag{2-12}$$

where $\rho_{\mu,N_\mu+1}(k)$ is the virtual downstream density of link μ of the virtual segment $N_\mu + 1$ at time step k. The quadratic term is used to account for the fact that one congested leaving link may block the entering link even if there is free flow in the other leaving link.

When a node has more than one entering links (e.g., at on-ramps), the influence of the upstream speeds has to be taken into account in Equation 2-3 (convection term of the equation) for the first segment $i = 1$ of link σ. To incorporate these upstream speeds, a so-called virtual upstream speed is defined as

$$v_{\sigma,0}(k) = \frac{\sum_{\mu\in\mathcal{I}_n} v_{\mu,N_\mu}(k)\cdot q_{\mu,N_\mu}(k)}{\sum_{\mu\in\mathcal{I}_n} q_{\mu,N_\mu}(k)} \tag{2-13}$$

where $v_{\sigma,0}(k)$ is the virtual upstream speed of leaving link σ of the virtual upstream segment 0 at time step k.

Extensions to the METANET model

A few extensions are proposed by Hegyi et al. [22] to model some parts of the traffic flow behavior in a more accurate way. The first extension is related to the control input variable speed limits. The original model was only built to describe the effect of ramp metering, and did not explicitly include the effect of variable speed limits. To describe the effect that this measure has on the traffic, the desired speed Equation 2-4 has been extended

$$V[\rho_{m,i}(k)] = \min\left[v_{\text{free},m}\cdot\exp\left[-\frac{1}{a_m}\left(\frac{\rho_{m,i}(k)}{\rho_{\text{crit},m}}\right)^{a_m}\right], (1+\alpha)u_{\text{vsl},m,i}(k)\right] \tag{2-14}$$

In this equation, the desired speed a vehicle wants to maintain depends on the minimum of two quantities. The first term describes the desired or equilibrium speed as a function of the density of that segment, whereas the second term ($u_{\text{vsl},m,i}(k)$) gives the maximum allowed speed for vehicles at that segment displayed on the variable message signs. This term is multiplied by the non-compliance factor $(1 + \alpha)$ that expresses the fact that drivers do not fully comply to the displayed maximum speed. From data of the Dutch freeways it is observed that when the speed limits are not enforced the average speed is higher than allowed ($\alpha = 0.1$), but when it is enforced the average speed is lower ($\alpha = -0.1$).

The second adaption made in the model is the expression for the different types of origin links. The behavior of traffic flow coming from an on-ramp is different compared to traffic coming from a mainstream origin. The mainstream origin can be affected by an active speed limit or by the actual speed on the first segment, whichever is smaller. So, for the inflow of the mainstream origin, Equation 2-8 is replaced by

$$q_o(k) = \min\left[d_o(k) + \frac{w_o(k)}{T_\mathrm{s}}, q_{\mathrm{lim},\sigma,1}(k)\right] \tag{2-15}$$

where the maximum flow $q_{\mathrm{lim},\sigma,1}$ is defined as

$$q_{\mathrm{lim},\sigma,1}(k) = \begin{cases} \lambda_\sigma \cdot v_{\mathrm{lim},\sigma,1}(k) \cdot \rho_{\mathrm{crit},\sigma}\left[-a_\sigma \ln\left(\frac{v_{\mathrm{lim},\sigma,1}(k)}{v_{\mathrm{free},m}}\right)\right]^{1/a_\sigma}, & \text{if } v_{\mathrm{lim},\sigma,1}(k) < V[\rho_{\mathrm{crit},\sigma}] \\ q_{\mathrm{cap},\sigma}, & \text{if } v_{\mathrm{lim},\sigma,1}(k) \geq V[\rho_{\mathrm{crit},\sigma}] \end{cases} \tag{2-16}$$

where the speed limit $v_{\mathrm{lim},\sigma,1}(k)$ is defined as the minimum of the actual speed on that segment and the maximum allowed speed displayed on the variable message signs

$$v_{\mathrm{lim},\sigma,1}(k) = \min\left[u_{\mathrm{vsl},\sigma,1}(k), v_{\sigma,1}(k)\right] \tag{2-17}$$

and the capacity flow $q_{\mathrm{cap},\sigma}$ is defined by

$$q_{\mathrm{cap},\sigma} = \lambda_\sigma V[\rho_{\mathrm{crit},\sigma}]\rho_{\mathrm{crit},\sigma} \tag{2-18}$$

Another modification of the model is made with respect to the boundary conditions for the upstream speed and downstream density, used to model the speed of the first and last segment of the traffic network in Equation 2-3. At a mainstream origin, the boundary condition for the speed of the virtual entering link will be set equal to the speed on the first segment

$$v_{\sigma,0}(k) = v_{\sigma,1}(k). \tag{2-19}$$

The boundary condition for the downstream density at the mainstream destination links, will be equal to the density of the last segment N_μ when traffic is in free flow and equal to the critical density when traffic is in congested flow:

$$\rho_{\mu,N_\mu+1}(k) = \begin{cases} \rho_{\mu,N_\mu}(k) & \text{if } \rho_{\mu,N_\mu}(k) < \rho_{\mathrm{crit},\mu} \\ \rho_{\mathrm{crit},\mu} & \text{if } \rho_{\mu,N_\mu}(k) \geq \rho_{\mathrm{crit},\mu} \end{cases} \tag{2-20}$$

The last modification is made with respect to the anticipation term used in Equation 2-3, to incorporate the different behavior of drivers when facing a positive or negative density difference downstream their segment. Drivers tend to anticipate more when a higher downstream density is present at the next segment with respect to their segment, than when a lower downstream density is present. To incorporate this anticipation difference, the anticipation constant ν is replaced by the anticipation constant η, where η takes the form

$$\eta_{m,i}(k) = \begin{cases} \eta_{\mathrm{high}}, & \text{if } \rho_{m,i+1}(k) \geq \rho_{m,i}(k) \\ \eta_{\mathrm{low}}, & \text{if } \rho_{m,i+1}(k) < \rho_{m,i}(k) \end{cases} \tag{2-21}$$

where η_{high} and η_{low} are, respectively, the anticipation constants for positive or negative difference with the downstream density.

2-2 Traffic emissions and fuel consumption models

In Section 2-1-2 the METANET model is described to estimate and predict the traffic flow on a macroscopic level. With this model the total time spent in the traffic network can be computed. However, to compute the traffic emissions and fuel consumption a second model is required. In this section some emissions and fuel consumption models are presented. Over the years a lot of models have been proposed to model the emissions and fuel consumption [48]. Due to the fact that emissions and fuel consumption depend on a lot of parameters a trade-off is often made in developing these models between the accuracy on the one hand and the required computation time on the other hand.

2-2-1 Overview of traffic emissions and fuel consumption models

Just as for traffic flow models the traffic emissions and fuel consumption models can be grouped according to their level of detail, where microscopic models are very detailed models and macroscopic models are coarse [27], [56], [58]. Basically, six groups of traffic emissions and fuel consumption models can be distinguished. In decreasing order of detail these groups are: modal models, cycle-variable based models, regression-based models, traffic-variable based models, traffic-situation based models, and average-speed based models [48]. These six types of models will be explained next.

- *Modal models.* In modal models the emission factors are computed via engine or vehicle operating models. The models are based on a simple parameterized physical and chemical process of a general vehicle system using functional modules. Therefore, these models require knowhow of detailed vehicle specifications and have relatively complex processes in different modules [12], [27]. Examples of modal models or power based models are CMEM [3], PHEM [19], four-mode elemental model [12], and CSIRO [12].
- *Cycle-variable models.* The emission in cycle-variable models depends on the driving cycle variables of vehicles at high time resolution (seconds to minutes) [48]. This type of models compute emission factors for different vehicle categories. Data is gathered from a large sample of vehicles that reflects the actual fleet composition [50]. A modal class is defined in terms of a unique combination of vehicle category and air pollutant. A vehicle category is defined e.g., in type of vehicle, fuel type, or fuel injection technology. The input needed for these type of models is the speed-time profile and vehicle specific parameters. Examples of cycle-variable models are MEASURE [18] and VERSIT+ [50].
- *Regression-based models.* In regression-based models the emission is computed via an empirical relationship between the emission and the product of speed and acceleration. Via regression the model is fitted to the data. The basic idea is that speed and acceleration can somehow represent the engine speed and power as independent variables. Examples of regression based emission models are VT-Micro [46], POLY [51], and VSP [16].
- *Traffic-variable models.* Traffic-variable emission models compute the emission factors based on a correction factor for the use of average speed. This type of models generate driving pattern data as a function of a number of macroscopic traffic variables, such

as traffic characteristics (flow, density, and speed) and road characteristics [41]. The core of the model is based on the reconstruction of the speed profile along a link where macroscopic traffic variables are provided. This approach considers traffic density as the fundamental physical reason of the variability of the speed of the vehicles, from which the time spent in acceleration, cruising, and idling, is calculated. Examples of traffic-variable models are TEE [41] and Matzoros model [38].

- *Traffic-situations based models.* In traffic-situations based models composite emission factors are determined for specific traffic situations, which are defined in terms of speed class, speed limit, and volume-to-capacity ratio (V/C ratio) to compute the emission levels. The amount of vehicle kilometers traveled per traffic situation is then multiplied by the corresponding emission factors. By integrating all the traffic situations the total emission of the traffic network can be computed. Examples of this type of models are HBEFA [20], ARTEMIS [28] and VERSIT+$^{\text{macro}}$ [49].

- *Average-speed based models.* The most simple type of emissions models is the average-speed based emissions models. These models are macroscopic models that use the average speed to compute the total vehiclular exhaust emissions. Typically, the input is the trip-based average speed but also local speeds can be used on a second-by-second basis [56]. Examples of macroscopic emission models are COPERT [34], MOBILE [15], and EMFAC [14].

In order to select the most appropriate model from this list of traffic emissions and fuel consumption models an assessment has been made, based on three criteria on which the models have to comply. First of all, the model has to be reasonably accurate. Change in acceleration and speed of vehicles should be incorporated in the model to efficiently control the emissions and fuel consumption. Secondly, the required computation time should not be too large, as the model needs to be applied in an on-line control approach. Thirdly, the emissions and fuel consumption model should be able to use the output of the traffic flow model METANET described in the previous section. From these requirements the class of regression-based models has been chosen, as these models take dynamic changes of speed and acceleration into account and as they are computationally less intensive than other microscopic emissions and fuel consumption models. From the regression-based models the VT-Micro model is selected. However, to integrate the VT-Micro model with the METANET model, the model is transformed from a microscopic into a macroscopic model. This new model is therefore called VT-Macro.

2-2-2 VT-Macro

VT-Macro [55] is a regression-based macroscopic emissions and fuel consumption model. It originates from the microscopic model VT-Micro [46], but has been altered in order to combine it with the traffic flow model METANET and to improve the computation speed. Therefore, first the concept of the VT-Micro model will be explained, after which the VT-Macro model will be derived.

VT-Micro

The Virginia Tech Microscopic (VT-Micro) model is a dynamic model that uses second-by-second speed and acceleration of a vehicle to compute its emissions and fuel consumption [46]. The basic idea is that speed and acceleration can somehow represent the engine speed and power as independent variables. The relationship of emissions and fuel consumption on the one hand and speed and acceleration on the other hand, is obtained by regression of the available data gathered from 9 vehicle categories that is assumed to represent the average vehicle on the road. This resulted in a third-order empirical relationship, which fits the data reasonably well. The emissions and fuel consumption cost $J_{\alpha,y}$ can now be computed via the equation

$$J_{\alpha,y}(l) = \exp(\tilde{v}_\alpha^T(l) P_y \tilde{a}_\alpha(l)) \tag{2-22}$$

where the subscript α stands for the vehicle under consideration, the subscript y stands for the type of emission or fuel consumption: $y \in \{\text{CO, NO}_x\text{, HC, fuel consumption}\}$, $\tilde{v}_\alpha(l) = \begin{bmatrix} 1 & v_\alpha(l) & v_\alpha^2(l) & v_\alpha^3(l) \end{bmatrix}^T$, and $\tilde{a}_\alpha(l) = \begin{bmatrix} 1 & a_\alpha(l) & a_\alpha^2(l) & a_\alpha^3(l) \end{bmatrix}^T$. Finally, P_y denotes the model parameter matrix for the variable y. The matrix is given in Appendix A-2. In this model the step counter l differs from the step counter used in the traffic flow model METANET, due to the difference in level of detail (microscopic versus macroscopic). Therefore, the time step T_m (microscopic) is introduced, such that $T_\text{m} \ll T_\text{s}$, where T_s is the macroscopic time step defined in Section 2-1-2. Typically, the time step T_m is around 1 s.

Note that the VT-Micro model does not describe the emission model for CO_2. However, it was found that the relationship between fuel consumption and CO_2 is almost affine and can be approximated by the equation

$$J_{\alpha,\text{CO}_2}(l) = \delta_1 v_\alpha(l) + \delta_2 J_{\alpha,\text{fuel}}(l) \tag{2-23}$$

In this equation, δ_1 and δ_2 are model parameters. For a diesel car the parameters take the values $1.17 \cdot 10^{-6}$kg/m and 2.65kg/L respectively, and for a gasoline car $3.5 \cdot 10^{-8}$kg/m and 2.39kg/L [55].

VT-Macro

The emissions and fuel consumption model VT-Micro is a microscopic model. This imposes some problems in the integration of VT-Micro and METANET. The output created by METANET is not rich enough to be used as input for the VT-Micro model. Recall that the macroscopic traffic flow model only uses aggregate variables, so only the average space-mean speed, flow, and density are computed per segment of the traffic network. However, the microscopic emissions and fuel consumption model needs the speed and acceleration of individual vehicles in a finer time grid. To overcome these problems the microscopic model VT-Micro has been rewritten into the macroscopic model VT-Macro [55]. The error introduced is qualified in the paper of Zegeye et al. [55].

In order to use the output of METANET to compute the corresponding emissions and fuel consumption, a transformation of these variables to the correct inputs for the VT-Macro model must be made. The flow, density, and speed of each segment must be transformed to the speed and acceleration of vehicles in that segment during that time step. Graphically, this transformation is represented in Figure 2-2. The METANET model is discrete both in

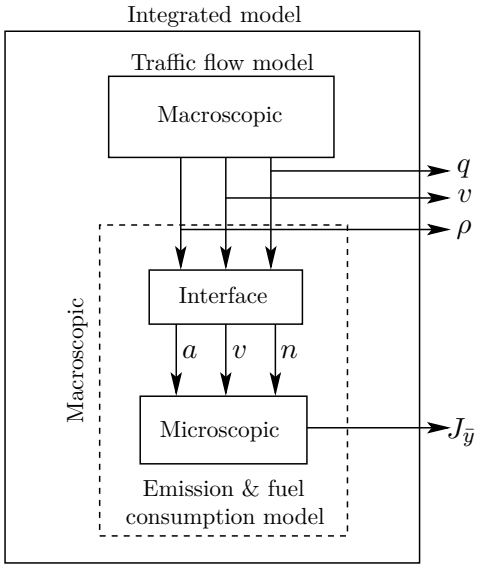

Figure 2-2: Interface block diagram

space and time, so there are two acceleration components involved in the model: temporal and spatiol-temporal acceleration. The first is the acceleration of the vehicles moving within a given segment. The second is the acceleration of the vehicles going from one segment to another from time step k to $k+1$. The average acceleration is computed for a group of vehicles. In Figure 2-3 the group of vehicles that enter or leave the segment is graphically represented. The emissions and fuel consumption computed by VT-Macro is equal to the emissions and fuel consumption computed by VT-Micro per vehicle for the average speed and acceleration multiplied by the number of vehicles that contributes to this emissions and fuel consumption.

Temporal acceleration

Temporal acceleration is described by the difference in speed in a segment during one time step. This acceleration is only computed for vehicles that stay in the segment for this time period. The temporal acceleration (a^{temp}) can be formulated as

$$a_{m,i}^{\text{temp}}(k) = \frac{v_{m,i}(k+1) - v_{m,i}(k)}{T_{\text{s}}} \tag{2-24}$$

The number of vehicles that stay in the segment can be determined as the number of vehicles present in the segment at time step k minus the amount of vehicles leaving the segment during the time period k till $k+1$. Mathematically, this is described by the formula

$$n_{m,i}^{\text{temp}}(k) = L_m \lambda_m \rho_{m,i}(k) - T_{\text{s}} q_{m,i}(k) \tag{2-25}$$

Spatio-temporal acceleration

Spatio-temporal acceleration can be described as the change in average speed experienced by going from one segment into another segment. If vehicles stay on the same link, then the

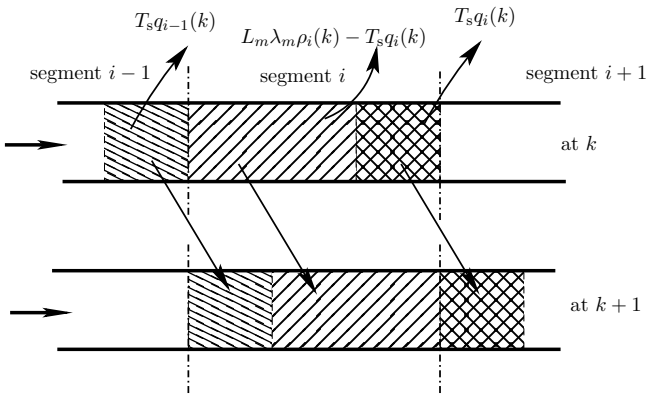

Figure 2-3: Graphical representation of the temporal and spatio-temporal displacement of vehicles from time step k to $k+1$

acceleration and number of vehicles can be described as

$$a^{\text{spat}}_{m,i,i+1}(k) = \frac{v_{m,i+1}(k+1) - v_{m,i}(k)}{T_s} \tag{2-26}$$

$$n^{\text{spat}}_{m,i,i+1}(k) = T_s q_{m,i}(k) \tag{2-27}$$

When the vehicles crosses a node during the considered time step, the spatio-temporal acceleration has to be computed in a different way. In general, the spatio-temporal acceleration of vehicles from the last segment N_μ of incoming link μ to the first segment of outgoing link σ can be computed by

$$a^{\text{spat}}_{\mu,\sigma}(k) = \frac{v_{\sigma,1}(k+1) - v_{\mu,N_\mu}(k)}{T_s} \tag{2-28}$$

The number of vehicles that enter link σ from link μ is determined by the turning rate $\beta_{\mu,\sigma}(k)$

$$n^{\text{spat}}_{\mu,\sigma}(k) = \beta_{\mu,\sigma}(k) q_{\mu,\sigma}(k) \tag{2-29}$$

This general form can be made case specific: vehicles coming from an on-ramp or going to an off-ramp or when a lane changes. These special cases are considered next.

- *On-ramp.* For on-ramps, the speed of the vehicles is not computed by METANET. Therefore, the formula of the general case cannot be used directly. The speed $v_{\text{on},o}(k)$ must be assigned to the vehicles, based on historical data when on-line measurements are not available. The formula of the general case then results in

$$a^{\text{spat}}_{\text{on},o}(k) = \frac{v_{m,i}(k+1) - v_{\text{on},o}(k)}{T_s} \tag{2-30}$$

$$n^{\text{spat}}_{\text{on},o}(k) = T_s q_{\text{on},o}(k) \tag{2-31}$$

  where $q_{\text{on},o}(k)$ is the flow at the on-ramp at time step k, given by the METANET model.

- *Off-ramp.* In the same way as the on-ramp, the off-ramp can be described. However, now the outflow $q_{\text{off},o}(k)$ is described as the fraction of vehicles that leave the freeway

$$q_{\text{off},o}(k) = \beta_{m,o}(k) q_{m,N_m}(k) \tag{2-32}$$

$$a^{\text{spat}}_{\text{off},o}(k) = \frac{v_{\text{off},o}(k+1) - v_{m,N_m}(k)}{T_{\text{s}}} \tag{2-33}$$

$$n^{\text{spat}}_{\text{off},o}(k) = T_{\text{s}} q_{\text{off},o}(k) \tag{2-34}$$

  in these equations $v_{\text{off},o}(k)$ is the speed of the vehicles leaving the network at the off-ramp at time step k. This speed is based on historical data or on-line measurements.

- *Lane drop/increase.* In case there is a lane drop or increase, the acceleration and number of vehicles can be determined by

$$a^{\text{spat}}_{m,m+1}(k) = \frac{v_{m+1,1}(k+1) - v_{m,N_m}(k)}{T_{\text{s}}} \tag{2-35}$$

$$n^{\text{spat}}_{m,m+1}(k) = T_{\text{s}} q_{m,N_m}(k). \tag{2-36}$$

The VT-Micro model can now be modified into a macroscopic emission model, VT-Macro, by using the temporal and spatio-temporal acceleration equations described above

$$J^{\text{temp}}_{y,m,i}(k) = n^{\text{temp}}_{m,i}(k) \exp[\tilde{v}^T_{m,i}(k) P_y \tilde{a}^{\text{temp}}_{m,i}(k)] \tag{2-37}$$

$$J^{\text{spat}}_{y,m,i,i+1}(k) = n^{\text{spat}}_{m,i,i+1}(k) \exp[\tilde{v}_{m,i}(k)^T P_y \tilde{a}^{\text{spat}}_{m,i,i+1}(k)] \tag{2-38}$$

$$J^{\text{spat}}_{y,\mu,\sigma}(k) = n^{\text{spat}}_{\mu,\sigma}(k) \exp[\tilde{v}_{\mu,\sigma}(k)^T P_y \tilde{a}^{\text{spat}}_{\mu,\sigma}(k)] \tag{2-39}$$

where $J^{\text{temp}}_{y,m,i}(k)$ denotes the temporal emission and fuel consumption of vehicles of type y of segment i of link m at time step k, $J^{\text{spat}}_{y,m,i,i+1}(k)$ denotes the spatio-temporal emission and fuel consumption of vehicles of type y that remain on the same link m at time step k, and $J^{\text{spat}}_{y,\mu,\sigma}(k)$ denotes the spatio-temporal emission and fuel consumption of vehicles of type y that cross a node from link μ to link σ at time step k.

Together, VT-Macro is described by Equations 2-37, 2-38 and 2-39:

$$\begin{aligned} J^{\text{EFC}}_y(k) = &\sum_{m \in \mathcal{M}} \sum_{i=1}^{N_m} J^{\text{temp}}_{y,m,i}(k) + \sum_{m \in \mathcal{M}} \sum_{i=1}^{N_m - 1} J^{\text{spat}}_{y,m,i,i+1}(k) \\ &+ \sum_{n \in \mathcal{N}} \sum_{\mu \in \mathcal{I}_n} \sum_{\sigma \in \mathcal{O}_n} J^{\text{spat}}_{y,\mu,\sigma}(k) \end{aligned} \tag{2-40}$$

where $J^{\text{EFC}}_y(k)$ is the emission and fuel consumption at time step k, $\mathcal{M}$ is the set of links m in the network, $\mathcal{N}$ is the set of nodes n in the network, $\mathcal{I}_n$ is the set of links that enter node n, and $\mathcal{O}_n$ is the set of links that leave node n.

The new VT-Macro model could be less accurate than the VT-Micro model, due to the approximation of the speed and acceleration of the individual vehicles. It is important to have an idea of how accurate the model has become. For that reason, Zegeye et al. [58] also included some analysis of VT-Macro, to compute the maximum error caused by the approximation of the speed and acceleration (for $T_{\text{s}} = T_{\text{m}}$). They found that a deviation of the acceleration and speed profile only introduces a minor error. In the scenario they conducted the maximal error was less than 10% compared to the VT-Micro model.

2-3 Summary and conclusions

This chapter has described the models that will be used to estimate and predict the traffic flow behavior as well as the corresponding emissions and fuel consumption. For the traffic flow behavior an extended version of METANET is selected. This is a second-order macroscopic traffic flow model. First it discretizes the traffic network in time and space. After that, it computes for each space segmentation the average flow, density, and space-mean speed for each time step. The model will be calibrated for the traffic network considered in the case study in Chapter 5.

The second model introduced in this chapter is the emissions and fuel consumption model VT-Macro. This model is a modification of the microscopic model VT-Micro, in order to use the output of the METANET model as input of the VT-Macro model and to reduce the computation time. Emissions and fuel consumption rates are hard to model, due to the dependency on a lot of parameters. Therefore, a trade-off has been made between the accuracy of the model and the computational effort. VT-Macro is selected, because it includes the dynamics of the vehicles (speed and acceleration) and still computes the emissions and fuel consumption on a macroscopic level. The error introduced by modifying the model from microscopic to macroscopic is relatively small compared to other macroscopic emissions and fuel consumption models. However, when more accurate models are available that require less computation time, these models could be used instead, to increase the efficiency of the dynamic controller.

Chapter 3

Model predictive control

In the previous chapter the models to estimate the traffic flow and the traffic emissions and fuel consumption based on a given traffic network and demand profile have been presented. This chapter will explain how these models can be used in an MPC framework to compute the control inputs (variable speed limits and ramp metering rates) that will steer the traffic flow into the desired direction. The structure of this chapter is as follows. First, a short introduction to the MPC control approach is presented in Section 3-1. Next, the concept of MPC and the methodology used in the case study are explained in Section 3-2 and 3-3 respectively. The chapter then provides an overview of the advantages and disadvantages of the approach in Section 3-4 and it concludes with a summary in Section 3-5.

3-1 Introduction

Model Predictive Control (MPC) is a control approach that computes the optimal control inputs that minimize a user-defined cost function over a prediction horizon without violating the constraints of the system. By optimizing the system over a predicted horizon, the controller is able to find an optimum over a long-term horizon, as the controller takes in advance into consideration the future (known) disturbances or changes of the states. It can also compute the effect of the measures it proposes to take over the predicted horizon. The MPC control approach was first successfully used in the process industry in the 1970s [47] and is a commonly used method for the control of slow dynamical systems such as chemical process control in the petrochemical, pulp, and paper industries [17], [29]. Nowadays MPC is used in all kind of different fields, ranging from robots to clinical anaesthesia [8]. In the recent years, research is conducted to see whether MPC is also applicable to (large-scale) traffic networks for on-line control of the travel time, emissions, and fuel consumption (see e.g., [22], [56], [55]). The study conducted in this thesis contributes to this research.

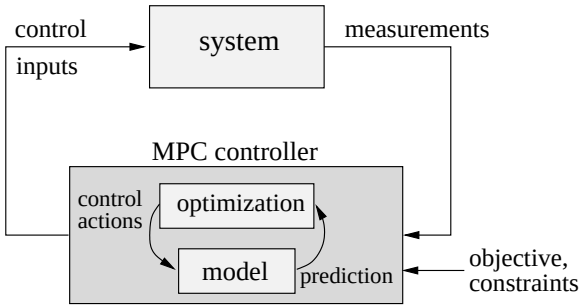

Figure 3-1: Block diagram of the concept of MPC

3-2 Concept of MPC

MPC is a model-based control approach that models the current and future states to find the optimal sequence of control inputs over time. The concept of the approach, as applied to traffic systems, can be explained by the block diagram depicted in Figure 3-1. Basically, the concept can be captured by the following five parts:

1. Traffic model
2. Objective of control approach
3. Constraints active on the system
4. Optimization of control inputs
5. Receding horizon principle

Part 1: Traffic model

The first part is to obtain an accurate description of the system. The models that will be used for this purpose are METANET and VT-Macro, as has been discussed in Chapter 2. Using these models, MPC is able to make an estimation of the traffic states based on the measurement data obtained by loop detectors in the road. When a demand profile of vehicles entering the network over some time horizon is available, MPC is able to make a prediction of the traffic states in the near future. The demand profile can be obtained by real data of previous days and/or estimated using data from upstream detectors. It is observed that the traffic demand profile is more or less the same for each weekday. For example, the morning rush hour of most days is around 7 till 9 A.M. [26]. Using this knowledge, a demand profile can be established that represents to some extent the actual demand. Another approach could be to use measurement data obtained from segments upstream of the considered traffic network. When the average speed and density upstream the traffic network is known, one can compute when these vehicles enter the traffic network. From this demand profile a prediction of the traffic states in the near future can be made, by applying the equations from the METANET and VT-Macro models.

Part 2: Objective of control approach

The next part is to determine the objective of the control approach and to transform it into a mathematical cost function. This objective could be anything related to the system, e.g., to prevent the formation of congestion, to increase the throughput of the traffic flow, or to reduce the amount of emissions produced by the vehicles over a period of time. When the objective is determined it has to be transformed to a cost function. This cost function relates the current and future traffic states to the objective by expressing the outcomes as a cost. By applying dynamic control inputs this cost function can be minimized, as the control inputs influence the predicted outcome of the traffic states. The transformation from the objective into a cost function will be explained in Section 3-3, where two different methodologies will be presented.

Part 3: Constraints active on the system

The third part is to include constraints that are active on the system. This could be all kinds of nonlinear time-varying constraints. Some obvious constraints are the upper and lower bounds of the control inputs. For example, variable speed limits could vary between 40 km/h and 120 km/h. The upper bound resembles the maximum allowed speed on freeways in The Netherlands, the lower bound resembles the lowest speed limits drivers still would comply to. For ramp metering rates the upper and lower bounds could be set between 1 and 0, as values beyond these bounds are simply not possible. Also other constraints could be set, for example a maximum queue length at on-ramps to prevent vehicles from spilling back to the local roads, a maximum allowed emission peak level, or a maximum variation of the control inputs over time and space.

The given constraints are so-called 'hard constraints'. The control approach is not allowed to violate these constraints. This will affect the degree of freedom of the controller, as not all possible control inputs are allowed anymore. Therefore, these constraints should be carefully placed, to avoid overconservatism of the control approach or even feasibility issues. To overcome the feasibility issues, some constraints could also be implemented in the cost function by using a penalty function. In this way, the constraints could be violated at the expense of some cost, emphasized by the weight in front of the criterion.

Part 4: Optimization of control inputs

Now that the cost function is defined and the constraints on the system are determined, the next part of the control approach is to find the optimal control inputs that minimize the cost function over the prediction horizon without violating the constraints. This is done using an optimization algorithm. For nonlinear local optimization algorithms, the minimum of a cost function is found iteratively by applying different sets of control inputs. Starting from an initial set of control inputs, the algorithm tries to find a new set of control inputs that results in a lower cost. This procedure is carried out until the algorithm cannot find a lower value for the cost function, i.e., when it reaches a minimum. However, when a system is nonlinear, this minimum could only be a local minimum instead of the global minimum. To increase the possibility of finding the global minimum, a multi-start optimization is used. The whole optimization needs to be solved again using a different set of initial control inputs. The lowest

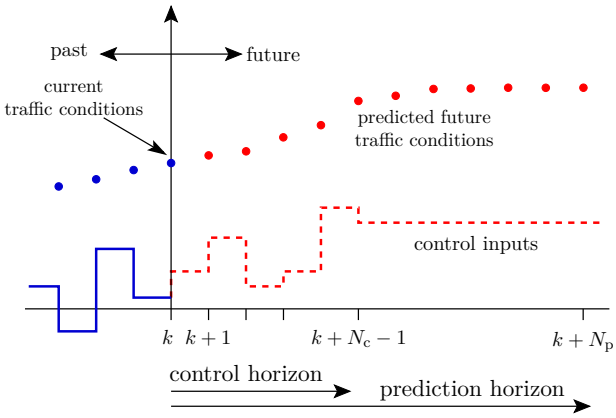

Figure 3-2: Receding horizon principle of the MPC approach. The approach computes the optimal path of the control inputs to steer the traffic flow in the desired direction, but only feeds the first set of control inputs to the real traffic system. The next time step, the optimization is carried out again. In this scheme also a control horizon is included. The approach varies the control inputs up to the control horizon, after which the control inputs remain constant.

minimum is then chosen from the set of minima. The optimization algorithms differs in the technique they use to derive a new set of control inputs.

Part 5: Receding horizon

When the optimal control inputs are determined, the set of control inputs that belongs to the current time step are fed to the real system. In the next control time step some new measurement data are available and the optimization of the control inputs is carried out again, using a shifted prediction horizon. This is called the receding horizon principle. This enables the MPC approach to counteract the model uncertainties and unknown disturbances that are present.

Because of the receding horizon principle, the MPC approach needs to be applied on-line, as it requires new measurement data at each control time step. Therefore, it is important that the required computation time for the controller is less than the duration of the control time step. Otherwise, the controller is not capable of sending the new set of control inputs to the real system at the next control time step.

Parameters of MPC

These five parts summarize the concept of the MPC approach. From this concept it has become evident that the approach depends on some parameters that can be tuned. First of all, the prediction horizon should be determined. A long prediction horizon enables the controller to optimize the traffic flow more efficiently, as this enables the controller to model the effect of its own measures on the traffic flow more completely [22]. However, the longer the prediction horizon, the more complex the optimization problem will be, resulting in higher computation times. Therefore, a balanced trade-off must be made for the choice of the length of the prediction horizon between the efficiency and the complexity of the approach. A guideline for the minimum length of the prediction horizon is the minimum time required for

vehicles to travel through the network [22].

To reduce the complexity of the optimization problem, a control horizon can be introduced in the MPC framework such that the control horizon is less than or equal to the prediction horizon. When a control horizon is present in the MPC framework, the approach may vary the control inputs up to the control horizon, after which the control inputs are kept constant till the prediction horizon. In this way, the algorithm only has to optimize the control inputs up to the control horizon, while the approach is still able to model the effects of the measures till the prediction horizon. This approach is shown in Figure 3-2.

Furthermore, the control time step, the type of optimization algorithm, and the number of multi-start points (if applicable), need to be determined. The control time step is the time between two consecutive steps where the controller can feed new control inputs to the system. As the loop detectors only provide measurement data once a minute, the control time step cannot be smaller than 1 minute. For higher values of the control time step the number of control inputs that needs to be optimized is reduced, but also the degree of freedom of the control approach. Again, a balanced trade-off must be made between efficiency and complexity. The control time step will be one of the tuning parameters in the case study.

The choice of the optimization algorithm depends on the optimization problem. Given the nature of the system (highly nonlinear and non-convex) there are a number of well-known optimization algorithms that can be applied, i.e., pattern search [4], genetic algorithms [11], simulated annealing [13], or sequential quadratic programming (SQP) [43]. For nonlinear local optimization algorithms a multi-start technique is required to increase the chance of finding the global minimum, instead of getting stuck in a local minimum. The number of required multi-start points depends on the complexity of the system, as the chance of finding the global minimum is lower for more complex systems than for simpler systems.

3-3 Methodology

As has been discussed in the concept of MPC, a user-defined objective must be given to the controller in the form of a cost function. The objective of the dynamic traffic controller could include all kinds of performance measures, such as the reduction of emissions, fuel consumption, or travel time. Another performance measure could be the inclusion of a penalty term on the variation of the control inputs to suppress chaotic behavior of the control inputs over time and space. Combining multiple performance measures leads to a multi-criteria cost function.

There are several ways to combine these performance measures into a cost function. In this section two ways are proposed. First, the weighted-sum method will be discussed, secondly, the ε-constraint method.

3-3-1 The weighted-sum method

In the weighted-sum method the different criteria of the objective are weighted by some user-defined weights. The sum of these weighted criteria is the cost function. The control approach aims to minimize this cost function by optimizing the control inputs that influences the cost function. To illustrate how the weighted-sum method handles multi-criteria cost functions,

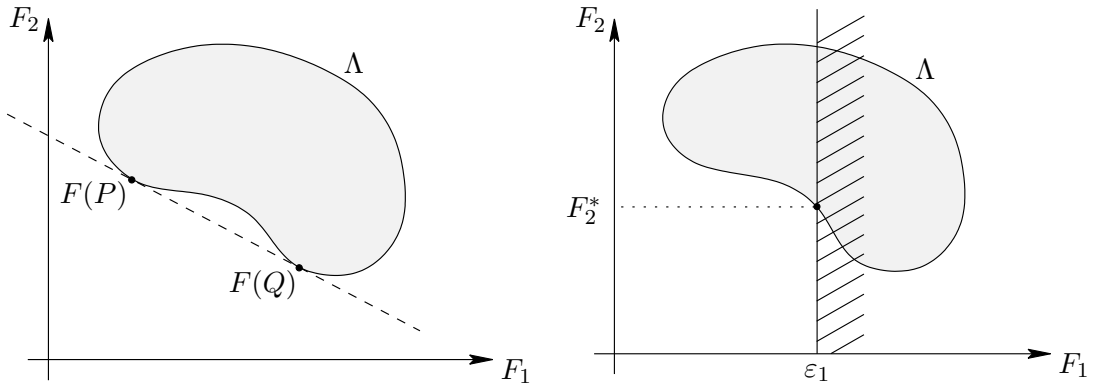

(a) Weighted-sum method (b) ε-constraint method

Figure 3-3: The weighted-sum method (a) and the ε-constraint method (b) for a non-convex solution boundary Λ.

an example with two criteria F_1 and F_2 will be considered. The cost function takes the form

$$J(k) = \alpha_1 \cdot \frac{F_1(k)}{F_{1,\mathrm{n}}} + \alpha_2 \cdot \frac{F_2(k)}{F_{2,\mathrm{n}}} \tag{3-1}$$

where $J(k)$ denotes the cost of the combined criteria at time step k, α_i are the user-defined weights for $i = 1, 2$, and $F_{1,\mathrm{n}}$ and $F_{2,\mathrm{n}}$ are the normalization values for F_1 and F_2, respectively. The functions are normalized to some value, so that the weights of the criteria are more easily tuned.

The choice for α_i determines the importance of each criterion in the cost function. For high values of α_1 compared to the value of α_2 the focus will lie more on that corresponding criterion. The choice for α_i can actually be seen as a policy decision. It is up to the policy makers to determine the importance of the criteria. Therefore, in this study a range of scenarios is explored to examine the effect of different weighting of the criteria. This can, e.g., be achieved by relating the weights as

$$\alpha_2 = 1 - \alpha_1 \tag{3-2}$$

with $\alpha_1 \in [0, 1]$.

This weighted-sum method seems to be a logical way of handling multiple criteria. However, this method also has some drawbacks. Applying the weighted-sum method does not give direct insight into the relationship between α_1 and the effect it has on the traffic flow. Only when a balanced trade-off curve is made, a sound choice for the weights can be made for that particular scenario. Another drawback is related to the non-convexity of the optimal trade-off curve. The optimal curve is the lower bound of the feasible region where the control inputs can vary in (solution boundary Λ). When this curve is non-convex (such as the curve depicted in Figure 3-3(a)) the weighted-sum method is not able to track all the possible optimal solutions by altering the weights. In this example, the region of the optimal curve between $F(P)$ and $F(Q)$ cannot be reached with the weighted-sum method. Therefore, another method is proposed that is able to deal with these issues. This method will be discussed in the next subsection.

3-3-2 The ε-constraint method

A second method to handle a multi-criteria cost function is the ε-constraint method. This method does not focus on the reduction of all the criteria at once, but focuses only on one criterion. In short, the method works as follows. Minimize one criterion such that the other criteria do not exceed some upper bound (see Figure 3-3(b)). In fact, this method considers the other criteria as hard constraints that may not be violated, while minimizing the primary criterion. To illustrate how this cost function would look like, the same example as for the weighted-sum method will be used. In this example the primary criterion will be set to F_1 and the secondary criterion to F_2.

$$\begin{aligned} J(k) &= F_1(k) \\ \text{such that } F_2(k) &\leq \varepsilon(k) \end{aligned} \tag{3-3}$$

Just as for the weighted-sum method the optimal control inputs depend on the choice for ε. The smaller ε is chosen, the more emphasis is placed on the constraints and the less freedom is left to reduce the primary criterion.

By expressing the cost function by the ε-constraint method the policy makers can directly see the effect of their decision for ε, because the constraint is a hard constraint that cannot be violated. Moreover, the issue of non-convexity is dealt with. However, this method also has a drawback. Whereas for the weighted-sum method it did not matter what value was chosen for α, it matters for the ε-constraint method. Too small values of ε could lead to feasibility issues where the control approach is not able to find any control inputs that satisfy the given constraints. In the case study presented in Chapter 5 the applied method will be the weighted-sum method to avoid this feasibility issue.

3-4 Advantages and disadvantages of MPC

The MPC approach discussed in Section 3-2 is well-suited for dynamic traffic control of freeways. There are a number of advantages of this control scheme [7], [23] compared to other control approaches such as iterative-learning based control [26], traditional optimal control [2], [33], or local control (demand capacity strategy, occupancy strategy, or ALINEA) [42]. The advantages are listed next.

- *Handle traffic systems.* MPC is able to deal with highly nonlinear time-varying systems. The behavior of the traffic flow, emissions, and fuel consumption fits this profile. By taking into account several future states the control approach is able to find an optimum that is suitable for a long-term horizon, instead of finding only a short-term optimum. Also, by combing several control measures over a whole network, a coordinated optimum can be found.
- *Handle a multi-criteria objective.* MPC can handle a multi-criteria objective, as has been shown in Section 3-3.
- *Handling constraints.* A major advantage of MPC that distinguishes MPC from other control approaches is its ability to handle constraints. The controller minimizes the objective function in an optimal way, such that it does not violate the constraints on

the model. Constraints could, for example, be the maximum queue length allowed on on-ramps.

- *Closed-loop structure.* MPC has a closed-loop structure as it uses a receding horizon principle. In this structure the traffic state and the current demands are fed back to the controller, so that the controller can handle disturbances in the demand or model errors. Traditional optimal controllers [33], however, have an open-loop structure. To be able to control the traffic flow in an optimal way, the disturbances must be known beforehand. Additionally, the traffic flow model must be very precise to ensure sufficient accuracy for the whole simulation.
- *Adaptivity.* It is easy to adapt the model during operation. This can be an advantage when major changes in the network have taken place. For example, when an accident occurs and a lane must be shut down, this can be easily adapted in the model during operation. Additional, the model itself can be updated once in a while.
- *Lower computation time.* MPC usually can suffice with a shorter prediction horizon, compared to traditional optimal controllers, which reduces the computation time, in general. This enlarges the feasibility of MPC controllers for on-line application.

The major drawback of the control approach MPC is the required computation time due to the complexity of the optimization problem. Although MPC is in general faster than other optimal control approaches due to the smaller prediction horizon and the control horizon [22], in many large-scale traffic networks it still is not fast enough to find the optimal control inputs to minimize the cost function. This drawback prevents the implementation of MPC in real large-scale traffic systems. Therefore, an alternative method needs to be developed to reduce the complexity of the problem. In this thesis such a method is developed by slightly altering the concept of the MPC approach. This will be explained in Chapter 4. Another drawback is the fact that the performance of MPC depends on the ability to predict the future demand accurately. The control inputs are optimized based on this prediction.

3-5 Summary

In this chapter, the control approach Model Predictive Control (MPC) is presented. In traffic systems, MPC makes an estimation and prediction of the current and future states of the system using models of the traffic flow, emissions, and fuel consumption. The approach optimizes the control inputs that influence the traffic states according to a user-defined cost function without violating the constraints that are active on the system. This optimization is achieved over a prediction horizon to find the optimal control sequence that minimizes the cost function. However, only the first set of control inputs corresponding to the current control time step are fed to the real system. At the next control time step, the whole optimization is carried out again with new received measurement data to counteract the presence of disturbances and model uncertainties.

Since the MPC control approach requires the description of a cost function, this chapter has presented a multi-criteria cost function. Two ways to define this cost function are presented, namely the weighted-sum method and the ε-constraint method. In the case study the weighted-sum method will be used as the method to define the cost function.

The advantages of an MPC control approach for dynamic traffic control are diverse. MPC can deal with the nonlinear time-varying traffic system, can handle the different operational and physical traffic constraints, multi-criteria cost functions, and disturbances, can be easily adapted to new traffic situations on-line, and optimizes the control inputs over a long-term horizon. However, the main issue for implementing this control scheme in the real traffic network is the limitation of the computation speed. To overcome this issue, an adaption is made to the concept of MPC, which will be explained in the next chapter.

Chapter 4

Parameterized MPC for traffic control

This chapter presents a variant of MPC, so-called parameterized MPC, that has lower computational requirements than conventional MPC. The chapter first provides a motivation for the parameterized MPC approach in Section 4-1, after which the general framework of the approach will be explained in Section 4-2. An example of the control laws used in the general framework in a traffic control context is given in Section 4-3. The chapter will conclude with a summary in Section 4-4.

4-1 Motivation

Conventional MPC, as described in Chapter 3, has many advantages that make it suitable for dynamic traffic control. However, for large-scale traffic networks the main limitation for on-line control is the required computation time due to the complexity of the optimization problem. This drawback prevents the control approach from being implemented in real-time applications of large-scale traffic networks. Therefore, a solution must be found to reduce the computational complexity of the optimization problem.

The required computation time largely depends on the optimization process of the control inputs over the prediction horizon. A nonlinear multi-start local optimization algorithm needs to find the optimal control values, in an iterative fashion, at each control time step over the prediction horizon. This procedure needs to be carried out multiple times to increase the chance of finding the global optimal set of control inputs, as the MPC optimization problem for traffic is nonlinear and nonconvex.

As have been discussed in Chapter 3, a common approach to reduce the complexity of the optimization problem is to use a control horizon N_{c}, such that the control horizon is less than the prediction horizon, i.e., $N_{\mathrm{c}} < N_{\mathrm{p}}$. The control inputs u_{ci} are allowed to vary only till the control horizon N_{c}, after which they remain constant till the prediction horizon N_{p} (see also Figure 3-2)

$$u_{\mathrm{ci}}(k + N_{\mathrm{c}} + j) = u_{\mathrm{ci}}(k + N_{\mathrm{c}} - 1) \tag{4-1}$$

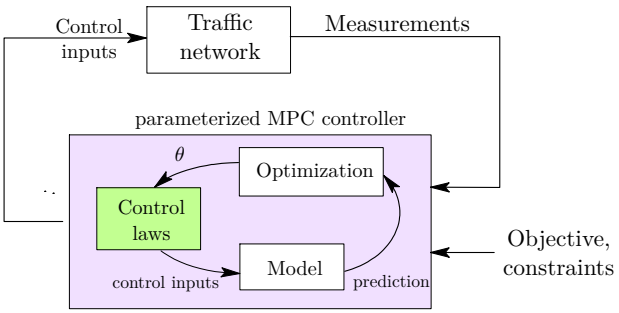

Figure 4-1: Block diagram of parameterized MPC

for $j = 0, \cdots, N_\mathrm{p} - N_\mathrm{c} - 1$. Thus the total number of control variables n_opt that has to be optimized is given by

$$n_\mathrm{opt} = n_\mathrm{i} \cdot (n_\mathrm{ci} \cdot N_\mathrm{c}) \tag{4-2}$$

where n_i is the number of multi-start points, n_ci is the number of control inputs, and N_c is the control horizon. The number of control inputs n_ci is defined as the sum of the number of independent variable speed limits n_vsl and the number of installed ramp meters at the on-ramps n_ro

$$n_\mathrm{ci} = n_\mathrm{vsl} + n_\mathrm{ro}. \tag{4-3}$$

By changing the number of multi-start points n_i, number of control inputs n_ci, or the control horizon N_c, the required computation time can be influenced. However, lowering these variables could also lead to a decrease in the performance of the controller to minimize a cost function. To maintain enough degree of freedom for the controller to steer the traffic flow these variables cannot be taken too small.

This chapter focuses on lowering the number of control inputs n_ci in the optimization problem. This can be achieved in several ways. One way is by splitting the traffic network into sub-networks, where for each sub-network a separate MPC controller is designed. The overall traffic network can be controlled by hierarchical control or agent-based control [22]. Another way is to group several variable speed limits over space (e.g., over a distance of 2 km the speed limits display the same value). However, this largely reduces the degree of freedom of the controller. Yet another way is to parameterize the control inputs [1], [57]. Instead of optimizing the control inputs directly, the optimization algorithm then optimizes the parameters of some user-defined control laws that are used to compute the control inputs. This approach will be studied in the remainder of this chapter.

4-2 General approach of parameterized MPC

In Figure 4-1 the concept of the parameterized MPC approach is given. Compared to the concept of conventional MPC as shown in Figure 3-1, the only difference of parameterized MPC with respect to conventional MPC is the way the optimization algorithm computes the optimal control inputs. Instead of directly optimizing the control inputs in the control approach, the optimization algorithm in parameterized MPC optimizes the parameters used

in the control laws. These control laws determine the corresponding control inputs. The whole strategy, as discussed in Chapter 3, remains the same. So, the control approach still optimizes the control inputs (indirectly, using control laws) that minimize a user-defined cost function under certain constraints, using an estimation and prediction of the real traffic flow, emissions, and fuel consumption computed by e.g. the METANET and VT-Macro models.

The control laws used in this block diagram relate the control inputs u_{ci} (variable speed limits and ramp metering rates) to the predicted traffic states $\hat{x}$ (density and speed) and predicted traffic outputs $\hat{y}$ (flow, travel time, emissions, and fuel consumption). The general form of such a control law is given by

$$u_{\text{ci}}(k_{\text{c}}+1+j'|k_{\text{c}}) = F\left(\hat{x}(k_{\text{c}}+j'|k_{\text{c}}), \hat{y}(k_{\text{c}}+j'|k_{\text{c}}), \theta(k_{\text{c}}+j'|k_{\text{c}})\right) \tag{4-4}$$

where $j' = 0, 1 \cdots, N_{\text{p}}-1$ and k_{c} denotes the control time step counter such that $u_{\text{ci}}(k_{\text{c}})$ is the time step where the new values of the control inputs are fed to the real system ($k = Mk_{\text{c}}$ for $M = T_{\text{c}}/T_{\text{s}}$). In the time between two control time steps the control inputs are kept constant. The function $F(\cdot)$ is a user-defined mapping that maps the predicted traffic states $\hat{x}(k_{\text{c}}+j'|k_{\text{c}})$, traffic outputs $\hat{y}(k_{\text{c}}+j'|k_{\text{c}})$, and parameter set $\theta(k_{\text{c}}+j'|k_{\text{c}})$ from the current time step up to the prediction horizon to the control inputs $u_{\text{ci}}(k_{\text{c}}+1+j'|k_{\text{c}})$, using information available at time step k_{c}.

The use of control laws to compute the control inputs introduces a new decision tool, the control policy. The control policy dictates the way the parameters of the control laws are allowed to vary over the prediction horizon. Basically, three control policies could be defined:

1. *Constant parameters.* The parameters of the control laws are kept constant throughout the entire prediction horizon ($\theta(k_{\text{c}}+j') = \theta(k_{\text{c}}), \forall j'$). This does not mean that the control inputs are constant over the prediction horizon, as they also depend on the traffic states and traffic outputs defined in the control laws.

2. *Variable parameters.* The parameters used in the control laws are time-varying over the prediction horizon. The control laws are, therefore, optimized every control time step to optimize the relation of control inputs and traffic states and traffic outputs.

3. *Combination of constant and variable parameters.* The parameters of the control laws are limited allowed to vary over the prediction horizon. This could be done by blocking the parameters over a predefined horizon, e.g., by using a control horizon, where the parameters are allowed to vary over the control horizon, but are kept constant from the control horizon till the prediction horizon.

The choice of the control policies influences the mapping of the function $F(\cdot)$ to the control inputs. The flexibility of the control laws to map the optimal sequence of control inputs is the largest for a variable control policy and the smallest for a constant control policy. The performance of the controller could therefore be less for a constant control policy than for a variable control policy. However, the number of control variables n_{opt} to be optimized is less for a constant control policy, which reduces the complexity of the optimization problem.

At every control time step the parameterized MPC approach optimizes the set of parameters used in the control laws described by the function $F(\cdot)$ to minimize the optimization

problem

$$\begin{aligned} \min_{\theta} J(k_c) &\equiv V(\mathbf{x}, \mathbf{y}, \theta, \mathbf{d}) \\ \text{subject to: } & g(\mathbf{x}, \mathbf{y}, \theta, \mathbf{d}) \leq 0, \\ & h(\mathbf{x}, \mathbf{y}, \theta, \mathbf{d}) = 0, \text{and} \\ & \text{system model} \end{aligned} \tag{4-5}$$

where $J(k_c)$ denotes the cost of applying the control inputs to the real system at time step k_c, $V(\mathbf{x}, \mathbf{y}, \theta, \mathbf{d})$ the user-defined cost function as a function of the traffic states $\mathbf{x}$, traffic outputs $\mathbf{y}$, parameter set θ, and the external inputs $\mathbf{d}$, all vectorized over the prediction horizon, and $g(\mathbf{x}, \mathbf{y}, \theta, \mathbf{d})$ and $h(\mathbf{x}, \mathbf{y}, \theta, \mathbf{d})$ are the inequality and equality constraint functions of the system.

Once the optimization algorithm is finished, the parameter set belonging to the current control time step $\theta(k_c|k_c)$ is used to compute the control inputs that needs to be fed to the real system. At the next control time step $k_c + 1$ the optimization algorithm is executed again, using the receding horizon principle, as discussed in Chapter 3.

4-3 Example of control laws

From the general framework presented in the previous section a range of control laws could be defined. In this section, two examples of the parameterization of the control inputs will be shown, one for each type of control inputs considered in this MSc thesis. In these examples the control laws are defined based on knowledge of traffic theory regarding the relation of the control inputs to the traffic states and traffic outputs.

4-3-1 Control law for variable speed limits

One of the primary objective of variable speed limits, as it is used in dynamic traffic control, is to prevent the formation of congestion [23]. Congestion occurs when the density of a segment exceeds the critical density. During congestion vehicles cannot drive at the maximum allowed speed without compromising the ability of vehicles to avoid collision. As a consequence, in case of a high demand upstream the congestion, more vehicles enter the dense segment than are able to leave. This increases the density and reduces the speed even more until the vehicles come to a complete stop at the maximum density. Variable speed limits are able to control to some extent the inflow of vehicles upstream to a dense segment, which leaves room for the dense segment to resolve the speed drop. Furthermore, variable speed limits can smoothen the speed variance between segments to prevent the creation of dense segments.

From this perspective, the variable speed limits can be linked to the current and predicted speed and density profiles of segments with respect to their neighboring segments. The following control law establishes this relation:

$$\begin{aligned} u_{\text{vsl},m,i}(k_c + j + 1) = \theta_0(k_c + j) \cdot u_{\text{vsl,max}} + \theta_1(k_c + j) \cdot \frac{v_{m,i+1}(k_c + j) - v_{m,i}(k_c + j)}{v_{m,i+1}(k_c + j) + \kappa_v} + \\ \theta_2(k_c + j) \cdot \frac{\rho_{m,i+1}(k_c + j) - \rho_{m,i}(k_c + j)}{\rho_{m,i+1}(k_c + j) + \kappa_\rho} \end{aligned} \tag{4-6}$$

where $u_{\text{vsl},m,i}(k_\text{c}+j)$ is the variable speed limit of segment i of link m at time step k_c for $j=0,\cdots,N_\text{p}-1$, $u_{\text{vsl,max}}$ is the maximum allowed speed of the traffic network, κ_v and κ_ρ are respectively the minimum non-zero speed and density model parameters, and $\theta_i(k_\text{c}+j)$ are the parameters to optimize for $i=0,1,2$ at time step k_c.

When the parameters $\theta_j(k_\text{c})$ are allowed to vary over the prediction horizon (variable control policy) the number of control variables n_opt that has to be optimized by the optimization algorithm from Equation 4-2 will be

$$n_\text{opt} = n_\text{i} \cdot (3 \cdot N_\text{c}) \tag{4-7}$$

regardless of the number of the variable speed limits compared to conventional MPC. The computational complexity is therefore reduced by this control law when the number of independent variable speed limits n_vsl is larger than 3.

When the parameters $\theta_j(k_\text{c})$ are kept constant over the prediction horizon (constant control policy) the number of control variables n_opt to be optimized is reduced even more to $3n_\text{i}$. In this scenario the computation complexity is already reduced if $n_\text{vsl} \cdot N_\text{c} > 3$.

4-3-2 Control law for ramp metering rates

Ramp metering is used to prevent the density of the freeways from exceeding a critical value ρ_crit, due to the merging behavior of vehicles from the on-ramp to the freeway. When the critical density is exceeded the throughput of the freeway and the average speed of the vehicles will drop. Therefore, the control law is defined such that the ramp metering rates are related to the density of the freeway near to the on-ramp and the critical density, which is here given by:

$$u_{\text{r},o}(k_\text{c}+j+1) = u_{\text{r,max}} + \theta_3(k_\text{c}) \cdot \frac{\rho_{\text{crit},m,1} - \rho_{m,1}(k_\text{c})}{\rho_{\text{crit},m,1}} \tag{4-8}$$

where $u_{\text{r},o}(k_\text{c})$ is the ramp metering rate at the on-ramp origin o at time step k_c, $u_{\text{r,max}}$ is the maximum ramp metering rate, and $\theta_3(k_\text{c})$ is the parameter at time step k_c.

When the parameter $\theta_3(k_\text{c})$ is allowed to vary over the prediction horizon (variable control policy) the number of control variables n_opt that has to be optimized by the optimization algorithm from Equation 4-2 will be

$$n_\text{opt} = n_\text{i} \cdot N_\text{c}. \tag{4-9}$$

The computation complexity is therefore reduced by this control law when the number of metered on-ramps n_ro is larger than 1.

When the parameter $\theta_3(k_\text{c})$ is kept constant over the prediction horizon the number of control variables n_opt to be optimized is equal to the number of multi-start points n_i, where the computation complexity is already reduced for $n_\text{ro} \cdot N_\text{c} > 1$.

4-3-3 General remarks concerning control laws

The control laws map the parameters to the control inputs. This mapping can reduce the flexibility of the control inputs to steer the traffic flow in the desired direction with respect

to the conventional MPC approach. Therefore, the control laws should be defined such that the remaining operational space of control inputs is close to the optimal values for the control inputs, to maintain a high level of performance compared to the conventional MPC approach.

The control laws presented are just one way to formulate the relationship of control inputs to the traffic states and traffic outputs. The given control laws can easily be altered to obtain other control laws. Also totally different control laws could be defined, based on the general formulation of control laws of Equation 4-4.

4-4 Summary

Parameterized MPC is introduced in order to reduce the computational complexity of the optimization problem of conventional MPC for large-scale traffic networks for on-line dynamic traffic control. To reduce the complexity of the optimization problem the number of control variables that have to be optimized, should be reduced. In parameterized MPC the control inputs are determined indirectly by user-defined control laws. The reduction of complexity can be realized when the number of parameters used in the control laws is less than the number of control inputs in parameterized MPC. A control law relates the control inputs to the traffic states and traffic outputs over the prediction horizon.

A general framework has been presented that can be used to define the control laws. From this general framework, a control law is defined for both types of control inputs considered in this MSc thesis, based on knowledge from traffic theory. The complexity of the optimization problem for traffic networks is reduced when more than three independent variable speed limits and more than one metered on-ramp are present for a variable control policy of the parameters. The complexity of the optimization problem is even much less when the constant control policy is chosen because the parameters do not change over the control horizon. Note, however, that the efficiency of the controller depends on the chosen control laws. Therefore, it is advisable to examine variations of these control laws or even completely different control laws.

Chapter 5

Case study

To test the MPC approach, and in particular the parameterized MPC approach, a case study is conducted. In Section 5-1 the set-up of the case study will be presented. Section 5-2 will describe the scenarios that are studied in this case study. In the remainder of the chapter the results of these scenarios will be presented for conventional MPC in Section 5-3 and parameterized MPC in Section 5-4, after which a comparison will be made between conventional and parameterized MPC in Section 5-5. The chapter concludes with a summary in Section 5-6.

5-1 Set-up of the case study

Prior to this thesis project, other case studies have been conducted on the Dutch A12 freeway between Bodegraven and Woerden (see e.g., [57]). For these studies, a calibrated METANET model was established of this particular part of the freeway. For that reason, the case study performed in this project is on the same site. The considered part of the A12 freeway is stretched between Bodegraven and Woerden (see Figure 5-1(a)). The total length of the freeway is approximately 15 km. The traffic network is divided into 3 links and 24 segments, as can be seen in Figure 5-1(b). The locations of the segments are chosen such that they match the place where a loop detector is located in the road. This slightly deviates from the METANET model presented in Chapter 2, where all segments within one link are of equal length. However, as long as the length of a segment is larger than the maximal length a vehicle travels within one time step, this does not matter for the model [31]. Furthermore, in the model the flow on the off-ramp is always considered to be at free-flow speed so that it does not affect the speed upstream the off-ramp, as was suggested in Section 2-1. The parameters of the extended METANET model and other case specific values are given in Appendix A.

A demand profile of one hour is defined (see Figure 5-2) to simulate a typical traffic flow on this part of the freeway at the end of the morning rush hour, using data of the traffic flow from January 23, 2006. As the traffic network has three entrances, the origin of the traffic network d_1 and the two on-ramps (d_2 at Waarder after approximately 3.3 km of the

(a) Site freeway between Bodegraven and Woerden (obtained from Google Maps)

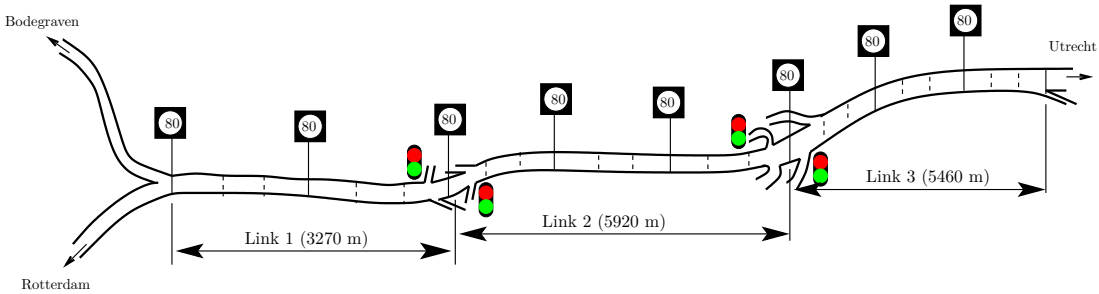

(b) Schematic representation of the location of the case study

Figure 5-1: Part of the Dutch A12 freeway (between Bodegraven and Woerden) of approximately 15 km length. The traffic network is discretized into 24 segments. It has two metered on-ramps and off-ramps (at Waarder and Linschoten). The variable speed limits are grouped per three segments.

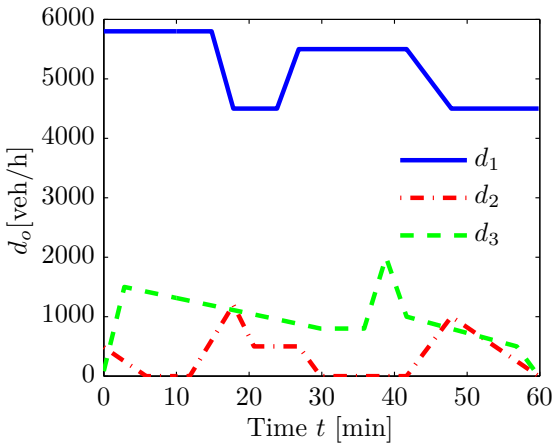

Figure 5-2: Demand profile for the origins used in the simulations based on real data obtained from the freeway. Demand d_1 is for the origin of the traffic freeway, demand d_2 for the first on-ramp, and demand d_3 for the second on-ramp.

traffic network and d_3 at Linschoten after approximately 9.2 km of the traffic network), the demand is split up into three demands corresponding to the location where the vehicles enter the traffic network. As can be seen in Figure 5-2 the main demand of vehicles comes from the origin of the traffic network, while a smaller portion of the demand comes from the on-ramps.

When the traffic network is not controlled by variable speed limits and ramp metering, the traffic flow would result in a congestion that spills back from the second on-ramp to the origin of the traffic network over time, for the given demand profile. This phenomenon can be observed in Figure 5-3. The congestion occurs directly after the start of the simulation in the vicinity of the second on-ramp and slowly spills back in a shock wave to the origin of the traffic network in a timespan of 40 minutes. As can be seen, from that moment on a queue starts to form at the origin of the traffic network, which is not yet resolved at the end of the simulation. The total time spent (TTS) of the vehicles in the traffic network during the simulation horizon is computed at 1136 vehicle hours. During this time, the total CO emission is estimated to be 190 kg and the total fuel consumption is estimated to be 7476 l. These values are set to be the normalization values for the controlled scenarios in order to see what the performance of the controlled scenario is compared to the uncontrolled scenario.

The control inputs considered in the controlled scenarios are the variable speed limits and the ramp metering rates (see Figure 5-1(b)). The variable speed limits are grouped per three segments to reduce the computation complexity of the controller and to prevent variations of the speed limits within a short distance. This means that, in the traffic network under consideration, there are eight independent variable speed limits that can be controlled. There are also two on-ramps located at this part of the A12 freeway. These on-ramps are metered by independent on-ramp metering installations. In total, the number of control inputs comes to $n_{\text{ci}} = 10$.

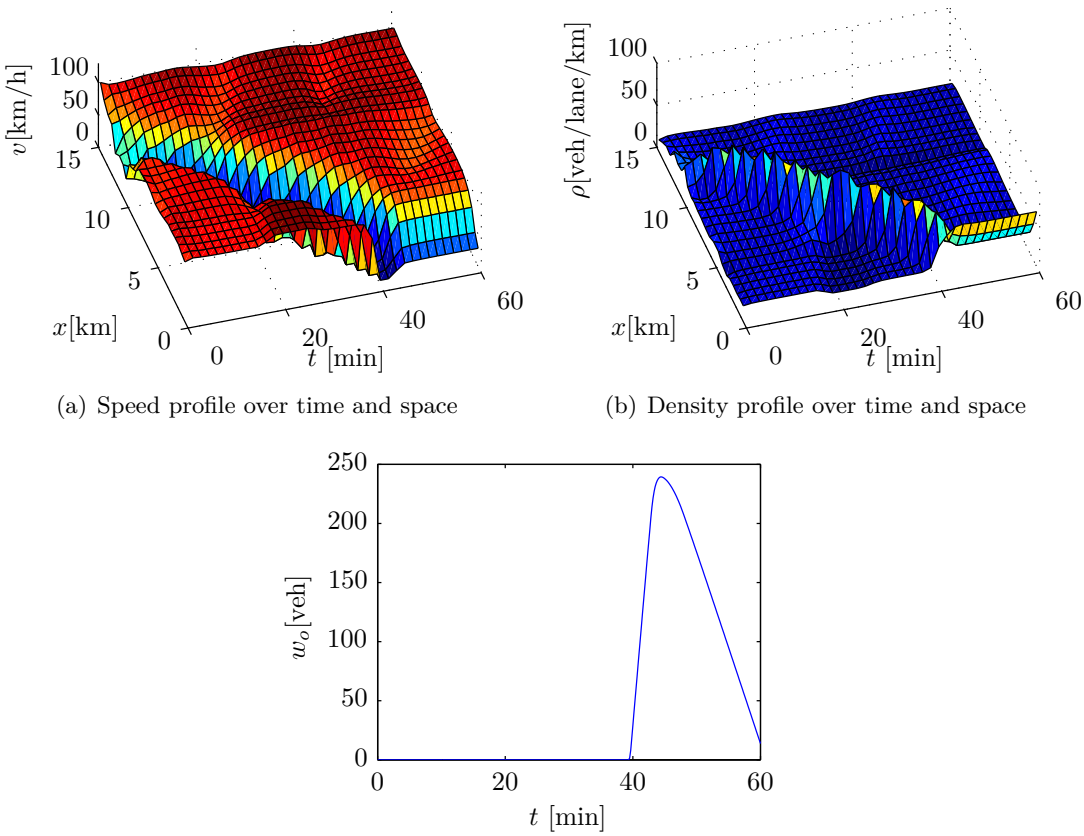

(a) Speed profile over time and space

(b) Density profile over time and space

(c) Queue length at origin of the traffic network

Figure 5-3: Speed and density profiles of the uncontrolled scenario over time t in min and space x in km. Congestion sets in immediately in the vicinity of the second on-ramp (approx. at 11 km) and spills back over time in a shock wave to the origin of the traffic network, after which a queue starts to form at that origin. During the simulation horizon of one hour, the congestion remains unsolved.

5-2 Scenario description

Based on the set-up of the case study presented in the previous section, the MPC controller can be used to compute the optimal control inputs to steer the traffic flow towards the desired direction. In this section, the scenario for the MPC approach will be described. First of all, the tuning parameters of the control approach are determined, after which the cost function and constraints are defined and the optimization algorithm is chosen.

5-2-1 Tuning parameters of MPC

The MPC approach has a few parameters for which appropriate values have to be selected. These tuning parameters influence the computational complexity and efficiency of the controller. The parameters for conventional MPC are the prediction horizon N_{p}, the control horizon N_{c}, the control time step T_{c}, and the number of multi-start points n_{i}, as presented in Chapter 3. For parameterized MPC two extra tuning parameters are introduced, the control policy and the bounds of the parameters θ used in the control laws, as discussed in Chapter 4.

- *Prediction and control horizon.* The prediction and control horizon are set to 15 min and 10 min, respectively. These values are used in previous studies [57] and have not been altered in this project.
- *Control time step.* The control time step is selected to be 5 min. At each control time step the controller can feed new optimal control inputs to the traffic network. The lower bound for T_{c} is 1 minute as this is the sample time interval at when new measurement data become available from the loop detectors. By increasing the control time step (e.g. from 1 to 5 min) the prediction horizon is reached within less steps, which reduces the complexity of the optimization problem. Furthermore, the variation of the control inputs over time is reduced, as it varies only once per 5 minutes. However, this comes at the expense of some performance loss of the controller, as the degree of freedom of the controller is lower.
- *Number of multi-start points.* The number of multi-start points for the optimization algorithm depends on the chosen optimization algorithm, the other tuning parameters, and on the selected control laws (for parameterized MPC). Since the considered optimization problem is highly nonlinear and nonconvex, in order to increase the chance of finding the global minimum the number of multi-start points is made larger. The number of multi-start points is varied in the range 5 to 150. This means that the optimization algorithm needs to be carried out at least 5 times in one control time step, to find the global minimum of the cost function. The set of initial values of the control inputs corresponding to the n^{th} optimization are set to

$$u_{\mathrm{initial}} = \begin{cases} \text{shifted} & 1^{\mathrm{st}} \\ \text{lower bounds} & 2^{\mathrm{nd}} \\ \text{upper bounds} & 3^{\mathrm{rd}} \\ \text{average of lower and upper bounds} & 4^{\mathrm{th}} \\ \text{random} & 5^{\mathrm{th}} \text{ and above} \end{cases} \tag{5-1}$$

where 'shifted' is the shifted optimal set of control inputs of the previous optimization. The lower and upper bounds are the lower and upper boundary values of the control inputs for conventional MPC and the lower and upper bounds of the parameters θ_i for parameterized MPC. To verify whether or not the number of multi-starts have been chosen correctly, a rule of thumb is that the global minimum should be found several times compared to the number of multi-start points. This is verified per controlled scenario and adapted were necessary. For conventional MPC the number of multi-start points is restricted to maximal 15, to limit the simulation time of the approach.

- *Control policy.* The control policy for parameterized MPC in this project differs between variable and constant values of the parameters θ of the control laws over the control horizon. At first, a variable control policy of the parameters of the control laws was chosen. Later on, the control policy was switched from variable to constant. Note that for a constant control policy the control inputs can still differ over the control horizon, due to the variation of the traffic states per segment.

- *Bounds of the parameters.* The upper and lower bounds of the parameters for parameterized MPC are less trivial to select. With conventional MPC the upper and lower bounds were defined as the physical bounds of the control inputs (see Equation 5-6). These bounds are, of course, still valid for the control inputs. However, theoretically the parameters of the control laws has no explicit bounds. This imposes a problem for the optimization algorithms to numerically find the optimal parameter values. Based on trial-and-error some bounds are selected in the simulations.

5-2-2 Cost function and constraints

Cost function

The objective of the dynamic traffic controller is to reduce the total time spent in the traffic network (TTS) and the total emissions and fuel consumption (TEFC). The corresponding multi-criteria cost function using the weighted-sum method is given by

$$J(k_c) = \alpha_1 \cdot \frac{\text{TTS}(k_c)}{\text{TTS}_n} + \alpha_2 \cdot \frac{\text{TEFC}(k_c)}{\text{TEFC}_n} \tag{5-2}$$

where TTS_n and TEFC_n are the normalization values for TTS and TEFC, respectively, and they are given by the values obtained previously for the uncontrolled scenario (see page 39), and α_1 and α_2 are the weight factors of the corresponding criteria. To determine the optimal weights for α_1 and α_2, a trade-off function is defined such that

$$\alpha_2 = 1 - \alpha_1 \text{ for } \alpha_1 \in [0, 1] \tag{5-3}$$

When $\alpha_1 = 0$ the focus lies completely on the reduction of emissions and fuel consumption; when $\alpha_1 = 1$ the focus lies completely on the reduction of the travel time. It is up to policy makers to decide which values for the weights are chosen, i.e. how much emphasis is placed on which criterion. With this trade-off function it is easy to implement different strategies over time.

The total time spent in the traffic network can be expressed as the total time vehicles

spent in the traffic network over the prediction horizon plus the total time vehicles spent in the queue at the origins during the prediction horizon. This is given by

$$\mathrm{TTS}(k_\mathrm{c}) = T_\mathrm{s} \cdot \sum_{k=Mk_\mathrm{c}}^{M(k_\mathrm{c}+N_\mathrm{p})-1} \left(\sum_{m\in\mathcal{M}} \sum_{i=1}^{N_m} \lambda_m L_{m,i} \rho_{m,i}(k) + \sum_{o\in\mathcal{I}_\mathrm{o}} w_o(k) \right) \tag{5-4}$$

where $L_{m,i}$ is the length of segment i of link m, λ_m is the number of lanes of link m, w_o is the queue length of origin o, $\mathcal{M}$ is the set of links of the traffic network, and $\mathcal{I}_\mathrm{o}$ is the set of origins of the traffic network.

The total emissions and fuel consumption can be expressed as

$$\mathrm{TEFC}(k_\mathrm{c}) = \sum_{k=Mk_\mathrm{c}}^{M(k_\mathrm{c}+N_\mathrm{p})-1} \sum_{y\in\mathcal{Y}} \gamma_y J_y^{\mathrm{EFC}}(k) \tag{5-5}$$

where γ_y is the weight for emissions or fuel consumption y, $\mathcal{Y}$ is the set of emissions and fuel consumption $\mathcal{Y} = \{\mathrm{CO}, \mathrm{HC}, \mathrm{NO}_x, \mathrm{FC}\}$, and $J_y^{\mathrm{EFC}}(k)$ is the emissions or fuel consumption y at simulation time step k as defined in Equation 2-40. To reduce the complexity of the system, the case study will focus on the reduction of carbon monoxide CO emissions.

Constraints

The constraints that are active on the system in the case study are the upper and lower bounds on the control inputs. The range for variable speed limits and ramp metering rates are, respectively, given by

$$\begin{array}{rcll} 40\,\mathrm{km/h} \leq & u_{\mathrm{vsl},m,i}(k) & \leq 120\,\mathrm{km/h} & \forall(m,i) \\ r_{\min} \leq & u_{\mathrm{r},o}(k) & \leq 1 & \forall o \in \mathcal{I}_\mathrm{o}. \end{array} \tag{5-6}$$

The lower bound of u_vsl is set to 40 km/h, because at this speed the freeway is considered to be congested, and congestion speed does not need to be displayed. Moreover, the legal minimum allowed speed of vehicles at freeways is 60 km/h when the freeway is not congested. Only during congestion vehicles may drive below this speed. The upper bound is set equal to the maximum allowed speed. In real applications this means that the variable message signs do not display a speed limit.

In the model the optimal variable speed limits can be every value between the upper and lower bound. However, the displayed message signs above the road only provide rounded values of the maximum allowed speed to the drivers (multiples of 10 km/h, for example 50 km/h or 70 km/h). The computed optimal speed limits should be rounded to a multiple of 10 km/h first, before they can be used by the displayed message signs. There are several ways to transform a continuous value to a discrete value, e.g., by ceiling, rounding, or flooring. In a study conducted in [23], the discretization of the continuous variable speed limits with the use of the commands 'ceil' and 'round' shows nearly the same performance as the continuous variable speed limits, but the command 'floor' shows poor performance. This is explained by the fact that the use of flooring results in overconservatism. It reduces the speed of vehicles too much, which leads to a lower throughput than would be the case in the scenario using the optimal control inputs. In this case study the command 'round' will be used to discretize the continuous speed limits computed by the optimization algorithm.

The bounds on the ramp metering rates resemble the physical range the rates can be in. The minimum $r_{\min}$ for the ramp metering rates is set to zero ($r_{\min} = 0$). When the ramp metering rate is zero, the traffic lights on the on-ramp display a red light during the entire cycle. When the ramp metering rate is one, the traffic lights on the on-ramp display a green light during the entire cycle. This is equal to an unmetered on-ramp. Values between zero and one allow a percentage of the vehicles to enter the freeway from the on-ramp.

5-2-3 Optimization algorithm

In the case study, the optimization toolbox of MATLAB® is used to minimize the multi-criteria cost function. More specifically, the command 'fmincon' is used for the optimization of the control inputs. This command can handle nonlinear and nonconvex optimization problems and can easily handle nonlinear time-varying constraints.

The built-in function 'fmincon' accepts three different algorithms, namely active-set, sequential quadratic programming (SQP), or interior-point. The algorithms differ in the way they compute the new set of control inputs. It is recommended to initially use the interior-point algorithm for large-scale problems. This results in more optimal control inputs than for the other two algorithms. However, it takes long computation time to converge to the optimal control inputs. Since the considered optimization problem is not a large-scale problem, the SQP algorithm can be selected, which is faster in convergence time. To reduce the computation time even more the active-set algorithm can be used. The interior-point and SQP algorithms satisfy the constraints at all time, while the active-set could violate the constraints in intermediary iterations. The active-set algorithm is faster, as it can take larger steps of the control inputs to converge to the optimal values.

For a more detailed overview of the differences in the algorithms, the website of The MathWorks Inc can be consulted [52], [53]. In the case study, both SQP algortihm and active-set algorithm of 'fmincon' has been used.

5-3 Conventional MPC

In the conventional MPC approach the traffic behavior is controlled by optimizing the set of control inputs over the prediction horizon to minimize the multi-criteria cost function without violating the constraints. For the scenario described in the previous sections, the results of the controller are presented in Figure 5-4 for $\alpha_1 = 1$ (focus on TTS reduction) and in Figure 5-5 for $\alpha_1 = 0$ (focus on CO reduction). The control time step T_c in these simulations is 5 minutes, the number of multi-start points n_i is 10 for $\alpha_1 = 1$ and 5 for $\alpha_1 = 0$, and the optimization algorithm is active-set.

As can be observed in Figure 5-4 the congestion that was initially formed at the second on-ramp is resolved within 10 minutes. During the remainder of the simulation the vehicles can drive (close to) the maximum allowed speed over the whole traffic network. The congestion was resolved by reducing the inflow to the traffic network at the second on-ramp. The ramp metering rate at that origin is kept low in the beginning, restricting vehicles from entering the already dense freeway. Obviously, this increases the queue length at that origin. However, this queue length is immediately reduced when the traffic density on the freeway allows more vehicles to enter the freeway without crossing the critical density. The TTS in the traffic

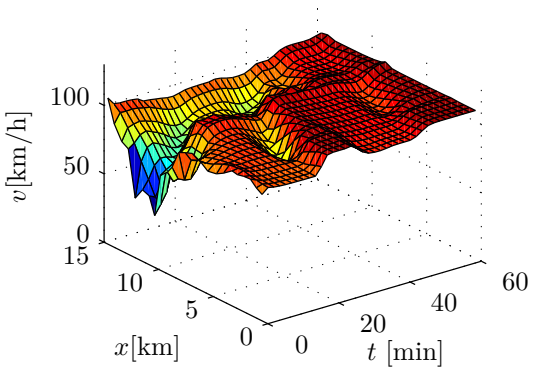

(a) Speed profile over time and space

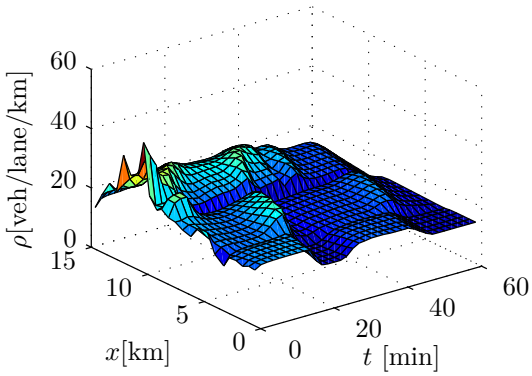

(b) Density profile over time and space

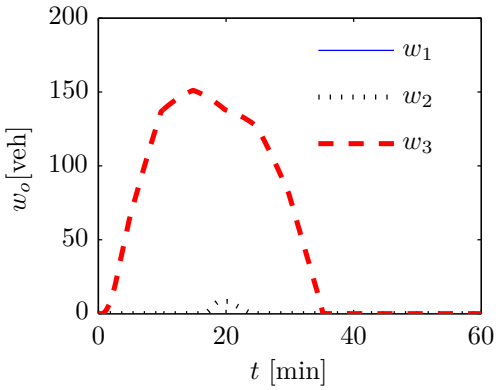

(c) Queue length at the origins over time

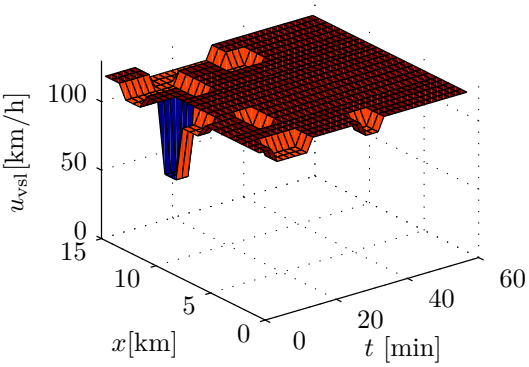

(d) Variable speed limits over time and space

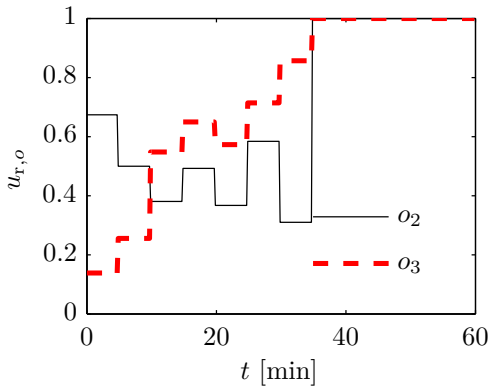

(e) Ramp metering rates over time

Figure 5-4: The evolution of the controlled freeway network over time and space for $\alpha_1 = 1$ (focus on TTS reduction) for conventional MPC. The congestion is resolved within 10 min, after which the average speed profile is above $90\,\mathrm{km/h}$. However, a queue starts to form at the second on-ramp w_3 of over 150 vehicles.

	TTS [veh · h]	TCO [kg]	TFC [l]	Computation time [min]
Uncontrolled	1136	190	7476	0
$\alpha_1 = 1.0$	902	215	7410	17.8
0.8	946	167	7013	8.2
0.6	1175	122	6830	10.3
0.4	2107	79	7322	13.7
0.2	2345	72	7478	6.7
0.0	2350	72	7485	4.4

Table 5-1: Effect of different weighting of the criteria for TTS, TCO, and TFC compared to the uncontrolled scenario for conventional MPC. The last column displays the maximum required computation time per control time step ($T_c = 5\,\text{min}$) of the whole simulation. Note that for $\alpha_1 = 1.0$ the number of multi-start points n_i is increased from 5 to 10 to obtain more optimal results.

network is reduced as a consequence of the optimal control inputs, however, at the cost of increased emissions and fuel consumption, as can be seen in Table 5-1.

When the focus of the controller is on the reduction of the carbon monoxide, as is shown in Figure 5-5, the controller tries to reduce the average speed of vehicles to approximately 50 km/h, as this is the optimal speed of vehicles with respect to the carbon monoxide emission. When vehicles drive faster or slower, the carbon monoxide emissions would rise. Logically, this increases the travel time dramatically. Due to the low allowed speed of vehicles imposed by the variable speed limits, the throughput is reduced and a queue will form at the origin of the traffic network. Obviously, this is not a proper solution for the reduction or prevention of congestion. Although the emissions are largely reduced in this scenario compared to the uncontrolled scenario, the travel time and fuel consumption are increased. In Table 5-1 the results for different weights of α_1 are shown for the total travel time (TTS), total carbon monoxide emissions (TCO), and total fuel consumption (TFC). Also, the maximum required computation time per control time step over the simulation horizon is given.

To show the relative improvement of the criteria with respect to the uncontrolled scenario, a trade-off curve is made in Figure 5-6 for the different weights of α_1. In this graph the relative improvement is computed as

$$\%\text{TTS} = \frac{\text{TTS}_\text{n} - \text{TTS}}{\text{TTS}_\text{n}} \cdot 100\% \tag{5-7}$$

$$\%\text{TEFC} = \frac{\text{TEFC}_\text{n} - \text{TEFC}}{\text{TEFC}_\text{n}} \cdot 100\% \tag{5-8}$$

where TTS denotes the travel time and TEFC denotes the total emissions and fuel consumption. From this curve, it can be observed that it is possible to reduce both the TTS and the TEFC at the same time for $\alpha_1 \in [0.65, 0.93]$, using the conventional MPC approach. In order to compute the optimal control inputs over the prediction horizon to minimize these criteria, the maximum computation time varied between 8 to 18 minutes per control time step (depending on the weights of α_1 and the number of multi-start points taken). Although the control time step has been increased in these simulation to 5 min, the conventional MPC approach still requires too much computation time. Therefore, the control approach cannot be implemented in real-life applications to control the traffic flow.

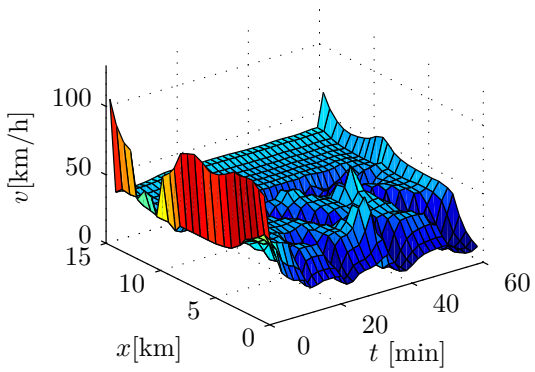

(a) Speed profile over time and space

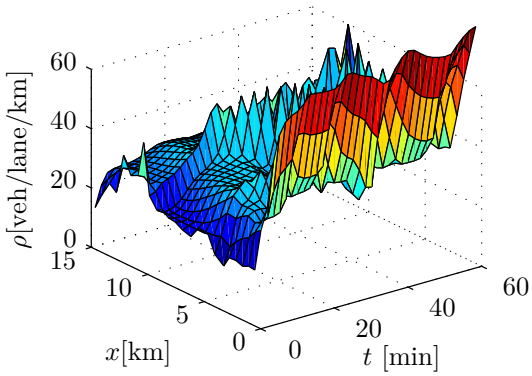

(b) Density profile over time and space

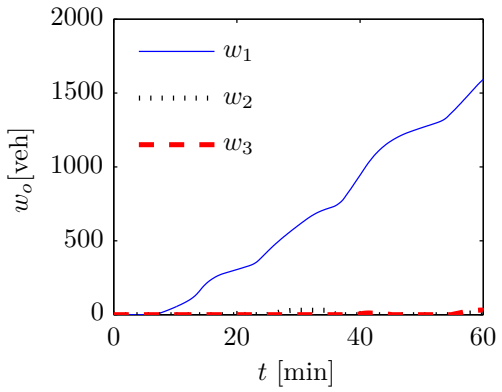

(c) Queue length at the origins over time

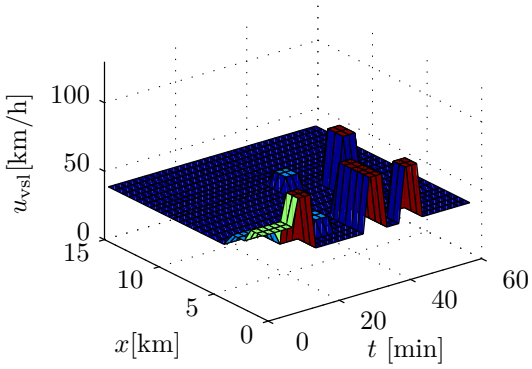

(d) Variable speed limits over time and space

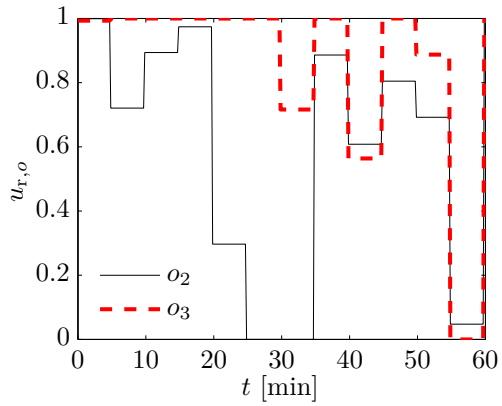

(e) Ramp metering rates over time

Figure 5-5: The evolution of the controlled freeway network over time and space for $\alpha_1 = 0$ (focus on CO emission reduction) for conventional MPC. The average speed of vehicles is reduced to $50\,\mathrm{km/h}$ to reduce the CO emission. At the origin of the traffic network a queue starts to form, due to the low allowed speed imposed by the speed limits.

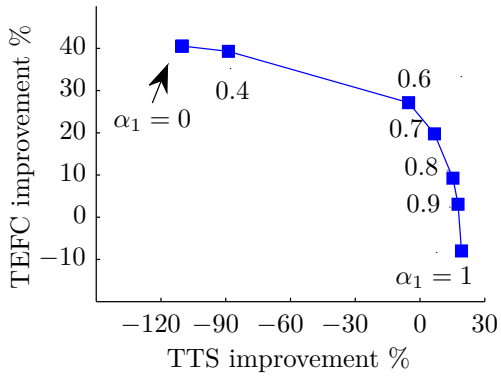

Figure 5-6: Relative improvement of the TTS and TEFC for different weights of α_1 for conventional MPC. For high values of α_1 the focus lies on the reduction of the TTS, which leads to an improvement of the TTS; for low values of α_1 the focus lies on the reduction of the TEFC, which leads to a reduction of the TTS.

5-4 Parameterized MPC

In the parameterized MPC approach, the variable speed limits and ramp metering rates are computed according to some user-defined control laws. These control laws relate the traffic states and traffic outputs to the control inputs. Basically, any kind of control law could be defined to parameterize the control inputs, as long as it satisfies Equation 4-4. In this case study, some control laws have been defined based on knowledge of the traffic behavior from traffic theory for each control measure; a few control laws that determine the variable speed limits and a few control laws that determine the ramp metering rates.

5-4-1 Control laws for variable speed limits

The control law for variable speed limits relates the variable speed limits to the traffic states speed and density. From traffic theory it is known that vehicles tend to reduce their speed when they encounter a high density downstream of their segment. Also, when the average speed of vehicles in the next segment is lower, drivers reduce their speed. One way to express this relation is given by the control law

$$u_{\text{vsl},m,i}(k_\text{c}+j+1) = \overbrace{\theta_0(k_\text{c}+j)\cdot u_{\text{vsl,max}}}^{A} + \overbrace{\theta_1(k_\text{c}+j)\cdot\frac{v_{m,i+1}(k_\text{c}+j)-v_{m,i}(k_\text{c}+j)}{v_{m,i+1}(k_\text{c}+j)+\kappa_\text{v}}}^{B} + \overbrace{\theta_2(k_\text{c}+j)\cdot\frac{\rho_{m,i+1}(k_\text{c}+j)-\rho_{m,i}(k_\text{c}+j)}{\rho_{m,i+1}(k_\text{c}+j)+\kappa_\rho}}^{C} \quad \text{(5-9)}$$

where $j = 0, \cdots, N_\text{p}-1$ and $u_{\text{vsl,max}}$ is the maximum allowed speed of the traffic network. Because of the difference in traffic speed and traffic density along the freeway, the variable speed limits can still vary over space while using this control law. In this way, all the independent variable speed limits are computed using the same equation. Instead of optimizing

every independent variable speed limit separately the optimization algorithm only has to optimize the parameters used in the control law. Note that the control policy in this equation is defined for variable parameters. For a constant control policy the parameters are given by $\theta_i(k_c + j) = \theta_i(k_c) \forall j$.

For this particular control law the variable speed limits depend on three terms. The first term A resembles the upper bound of the variable speed limits. The second term B consists of the relative speed difference between two consecutive segments i and $i+1$. The third term C consists of the relative density difference of two consecutive segments i and $i+1$. Of course, the defined control law is just one way to express the relation of the variable speed limits with the traffic states. Other control laws for variable speed limits can be obtained, for example, by varying the terms A, B, and C. In this case study, the following variations are examined:

$$A_p = \theta_0(k_c + j) \cdot \begin{cases} u_{\text{vsl,max}} & p = 1 \\ u_{\text{vsl},m,i}(k_c + j) & p = 2 \end{cases}$$

$$B_p = \theta_1(k_c + j) \cdot \begin{cases} \dfrac{v_{m,i+1}(k_c + j) - v_{m,i}(k_c + j)}{v_{m,i+1}(k_c + j) + \kappa_v} & p = 1 \\ v_{m,i+1}(k_c + j) - v_{m,i}(k_c + j) & p = 2 \\ \dfrac{\frac{1}{2}(v_{m,i+2}(k_c + j) + v_{m,i+1}(k_c + j)) - v_{m,i}(k_c + j)}{\frac{1}{2}(v_{m,i+2}(k_c + j) + v_{m,i+1}(k_c + j)) + \kappa_v} & p = 3 \\ \dfrac{V[\rho_{m,i}(k_c + j)] - v_{m,i}(k_c + j)}{V[\rho_{m,i}(k_c + j)] + \kappa_v} & p = 4 \\ \dfrac{v_{m,i+1}(k_c + j) \cdot \rho_{m,i+1}(k_c + j) - v_{m,i}(k_c + j) \cdot \rho_{m,i}(k_c + j)}{v_{m,i+1}(k_c + j) \cdot \rho_{m,i+1}(k_c + j) + \kappa_v \cdot \kappa_\rho} & p = 5 \end{cases}$$

$$C_p = \theta_2(k_c + j) \cdot \begin{cases} \dfrac{\rho_{m,i+1}(k_c + j) - \rho_{m,i}(k_c + j)}{\rho_{m,i+1}(k_c + j) + \kappa_\rho} & p = 1 \\ \rho_{m,i+1}(k_c + j) - \rho_{m,i}(k_c + j) & p = 2 \\ \dfrac{\frac{1}{2}(\rho_{m,i+2}(k_c + j) + \rho_{m,i+1}(k_c + j)) - \rho_{m,i}(k_c + j)}{\frac{1}{2}(\rho_{m,i+2}(k_c + j) + \rho_{m,i+1}(k_c + j)) + \kappa_\rho} & p = 3 \end{cases}$$

Option A_2 is the variable speed limits of the previous control time step. By replacing the maximum allowed speed by the previous variable speed limits, the variation between variable speed limits over time is limited. Option B_2 and C_2 are a simplification of the primary control law (no division of the differences). Option B_3 and C_3 are an extension of the speed and density differences with an additional downstream segment. Option B_4 considers the speed differences with the desired speed and the current speed of that segment. Finally, option B_5 is the difference of the product of the speed and density between two consecutive segments.

In total, this case study considers seven control laws for variable speed limits by combining

some of the possible variations described above:

$$
\begin{aligned}
u_{\text{vsl},m,i}(k_\text{c}+j+1) &= A_1 + B_1 + C_1 \\
u_{\text{vsl},m,i}(k_\text{c}+j+1) &= A_2 + B_1 + C_1 \\
u_{\text{vsl},m,i}(k_\text{c}+j+1) &= A_1 + B_2 + C_2 \\
u_{\text{vsl},m,i}(k_\text{c}+j+1) &= A_1 + B_3 + C_3 \\
u_{\text{vsl},m,i}(k_\text{c}+j+1) &= A_1 + B_4 + C_1 \\
u_{\text{vsl},m,i}(k_\text{c}+j+1) &= A_1 + B_4 \\
u_{\text{vsl},m,i}(k_\text{c}+j+1) &= A_1 + B_5
\end{aligned}
$$

In the first five combinations the number of parameters used in the control law in reduced to three, in the last two combinations even to two. Recall that in the conventional MPC approach, the number of independent variable speed limits was set to eight. So, the number of control variables is reduced with a factor of $2.7 - 4$ for the considered speed limits for the variable control policy and even more for the constant control policy (extra factor 2 for $T_\text{c} = 5\,\text{min}$ and $N_\text{c} = 10\,\text{min}$).

5-4-2 Control laws for ramp metering rates

The control law for ramp metering rates is defined based on congestion prevention in the vicinity of on-ramps. From traffic theory it is known that the maximal capacity q_max on a freeway is reached at the critical density ρ_crit. When a higher traffic density is formed, the speed of vehicles will drop and less vehicles can flow through the traffic network. To prevent congestion the density of vehicles in the vicinity of on-ramps should be kept below the critical density. This is translated in the control law

$$
u_{\text{r},o}(k_\text{c}+j+1) = \overbrace{u_{\text{r},o}(k_\text{c}+j)}^{D} + \overbrace{\theta_3(k_\text{c}+j) \cdot \frac{\rho_\text{crit} - \rho_{m,1}(k_\text{c}+j)}{\rho_\text{crit}}}^{E} \tag{5-10}
$$

where $u_{\text{r},o}(k_\text{c}+j)$ denotes the previous ramp metering rate at on-ramp o and $\rho_{m,1}$ is the density of the first segment of the link m connected to on-ramp o. To reduce the number of parameters compared to the conventional MPC approach, only one parameter is used to parameterize the control law for ramp metering rates. For this reason, there is no parameter in front of term D as was the case in the control law for variable speed limits (term A). Just as for the control law for variable speed limits, several variations are made of the control law

for ramp metering rates:

$$D_p = \begin{cases} u_{\mathrm{r},o}(k_\mathrm{c}+j) & p=1 \\ u_{\mathrm{r,max}} & p=2 \end{cases}$$

$$E_p = \theta_3(k_\mathrm{c}+j)\cdot \begin{cases} \dfrac{\rho_\mathrm{crit}-\rho_{m,1}(k_\mathrm{c}+j)}{\rho_\mathrm{crit}} & p=1 \\ \dfrac{\rho_\mathrm{crit}-\frac{1}{2}(\rho_{m,2}(k_\mathrm{c}+j)+\rho_{m,1}(k_\mathrm{c}+j))}{\rho_\mathrm{crit}} & p=2 \\ \dfrac{\rho_\mathrm{crit}-\frac{1}{2}(\rho_{\mu,N_m}(k_\mathrm{c}+j)+\rho_{m,1}(k_\mathrm{c}+j))}{\rho_\mathrm{crit}} & p=3 \end{cases}$$

where link m is connected to the on-ramp o and link μ is the link upstream link m. Option D_2 is the upper bound of the ramp metering rate. Option E_2 includes an extra segment upstream of the on-ramp in the density differences. Option E_3 includes an extra segment downstream of the on-ramp in the density differences. In this case study four combinations of D and E are considered:

$$\begin{aligned} u_{\mathrm{r},o}(k_\mathrm{c}+j+1) &= D_1+E_1 \\ u_{\mathrm{r},o}(k_\mathrm{c}+j+1) &= D_2+E_1 \\ u_{\mathrm{r},o}(k_\mathrm{c}+j+1) &= D_1+E_2 \\ u_{\mathrm{r},o}(k_\mathrm{c}+j+1) &= D_1+E_3 \end{aligned}$$

.

The simulations are carried out in two stages. In the first stage, the variable speed limits are parameterized using one of the seven variations of the control law described before. In this stage, the ramp metering rates are not parameterized, but are still optimized using the conventional MPC approach. This is mainly done in order to test the control laws of each control measure separately. The second stage includes the parameterization of both the control measures in the parameterized MPC approach. As it is the goal in this stage to test the effect of the variation of the control law for ramp metering rates, one and the same control law for variable speed limits is used, namely $u_{\mathrm{vsl},m,i}(k_\mathrm{c}+j+1) = A_1+B_1+C_1$.

5-4-3 Results of parameterized MPC

Using the control laws described above, the parameterized MPC approach is able to resolve the formation of congestion for the scenario described in Section 5-1. This can be observed in Figures 5-7, 5-8, and 5-9, where the speed, density, and queue profiles are shown, together with the corresponding optimized values of the parameters θ_i and the resulting control inputs for two variations of the control laws.

In the first simulation, only the variable speed limits are parameterized using the control law $u_{\mathrm{vsl},m,i}(k_\mathrm{c}+j+1) = A_1+B_4$, while the ramp metering rates are still optimized using the conventional MPC approach. The optimization algorithm is SQP, the number of multi-start points is 20, the control time step is 5 min, the control policy is constant parameters, and the bounds of the parameters are ± 1 for θ_0 and ± 200 for θ_1. The result is shown for $\alpha_1 = 1$ (focus on TTS reduction) in Figure 5-7.

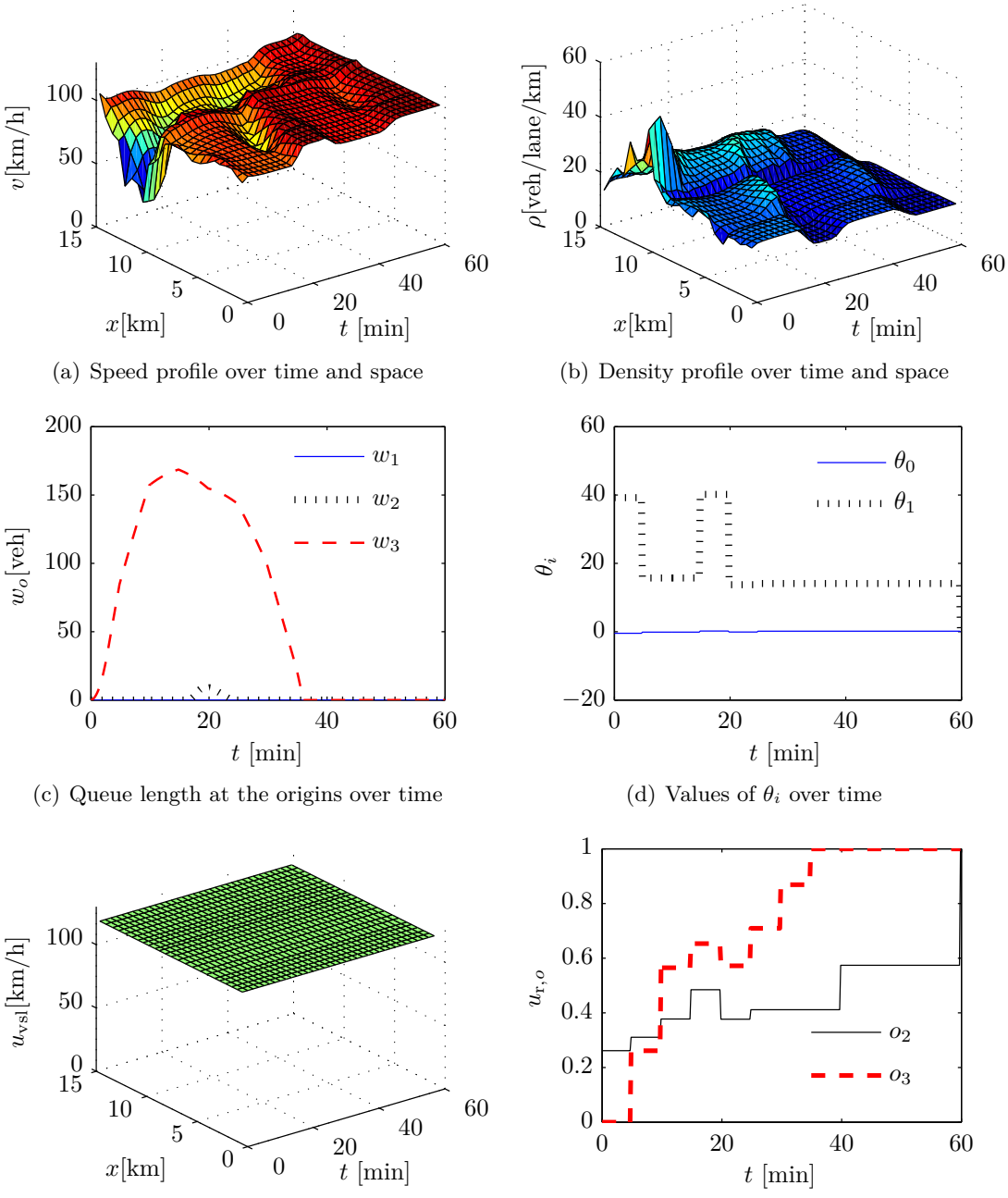

(a) Speed profile over time and space

(b) Density profile over time and space

(c) Queue length at the origins over time

(d) Values of θ_i over time

(e) Variable speed limits over time and space

(f) Ramp metering rates over time

Figure 5-7: The evolution of the controlled freeway network over time and space for $\alpha_1 = 1$ (focus on TTS reduction) for parameterized MPC for variable speed limits and conventional MPC for ramp metering rates. The congestion at the second on-ramp is resolved within a few minutes, however, the density remains somewhat high in that region compared to the solution with the conventional approach. The congestion is resolved at the expense of a queue of over 150 vehicles at the second on-ramp.

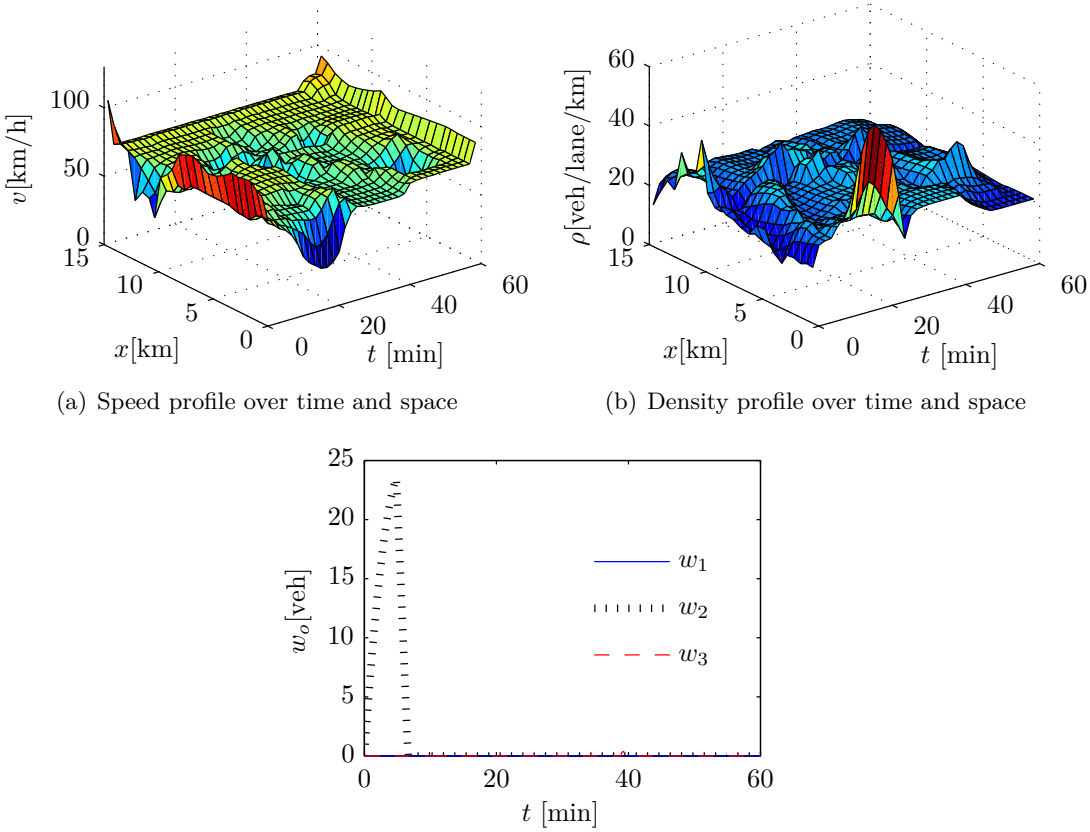

(a) Speed profile over time and space

(b) Density profile over time and space

(c) Queue length at the origins over time

Figure 5-8: The evolution of the controlled freeway network over time and space for $\alpha_1 = 0.6$ (focus partly on TTS reduction and partly on CO reduction) for parameterized MPC for both control measures. The congestion in the vicinity of the second on-ramp is resolved, but the average speed does not rise to the maximum allowed speed due to the inclusion of the CO emission in the cost function. Only a minor queue is formed at the first on-ramp.

The speed and density profiles show that the control approach is able to resolve the congestion that was initiated at the second on-ramp. The use of ramp metering for the control of the traffic network is sufficient to resolve the congestion, resulting in a queue at the second on-ramp. The values of the parameters are chosen such that the variable speed limits are constant at 120 km/h.

The second simulation shown here is the result of the parameterized MPC approach for the control laws $u_{\text{vsl},m,i}(k_c+j+1) = A_1+B_1+C_1$ and $u_{\text{r},o}(k_c+j+1) = D_1+E_1$. In this simulation, both control measures are parameterized. The optimization algorithm is active-set, the number of multi-starts is 10, the control time step is 5 min, the control policy is constant parameters, and the bounds of the parameters are ± 1 for θ_0, ± 200 for θ_1 and θ_2, and ± 50 for θ_3. The result is shown for $\alpha_1 = 0.6$ (focus partly on TTS reduction and partly on CO reduction) in Figure 5-8 and Figure 5-9.

From the speed, density, and queue plots in Figure 5-8 it can be seen that the congestion at the second on-ramp is resolved at the beginning of the simulation. The average speed does not go to the maximum allowed speed, as the controller also takes into account the effects of

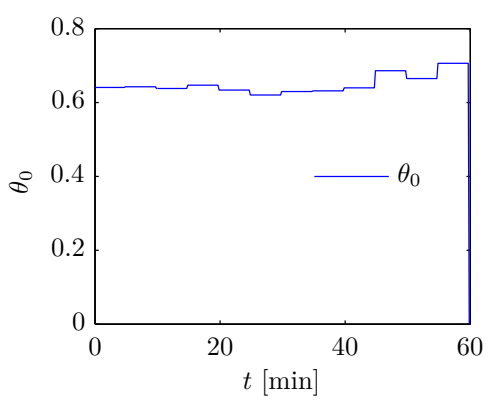

(a) Values of θ_0 over time

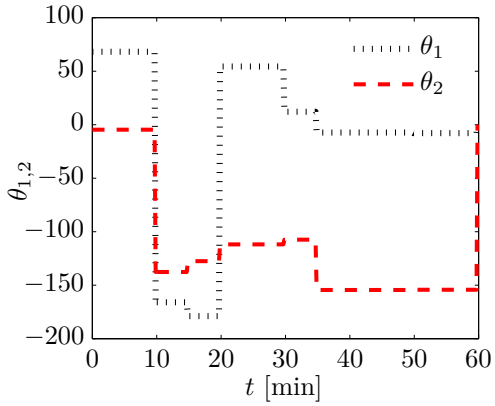

(b) Values of θ_1 and θ_2 over time

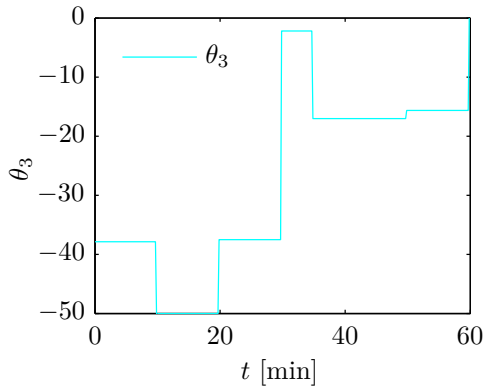

(c) Values of θ_3 over time

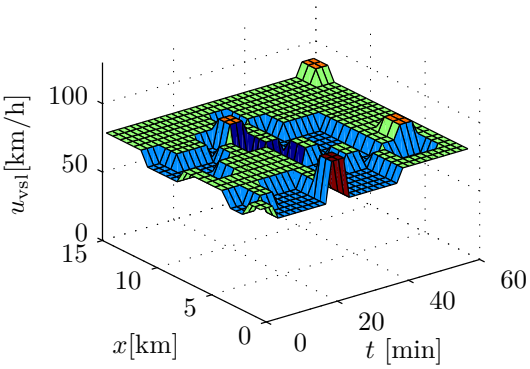

(d) Variable speed limits over time and space

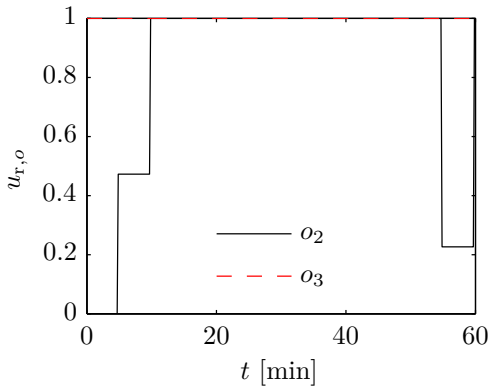

(e) Ramp metering rates over time

Figure 5-9: Evolution of the parameters of the control law $u_{\text{vsl},m,i}(k_c + j + 1) = A_1 + B_1 + C_1$ and the control law $u_{r,o}(k_c + j + 1) = D_1 + E_1$ over time, with the corresponding variable speed limits and ramp metering rates.

$u_{\text{vsl},m,i}(k_c+j+1)$		TTS [veh · h]	TCO [kg]	TFC [l]	Computation time [min]
Uncontrolled		1136	190	7476	0
Conventional	$\alpha_1 = 1$	902	215	7410	17.8
$A_1 + B_1 + C_1$		903	216	7422	1.1
$A_2 + B_1 + C_1$		911	217	7448	2.8
$A_1 + B_2 + C_2$		903	215	7413	1.0
$A_1 + B_3 + C_3$		911	217	7449	1.3
$A_1 + B_4 + C_1$		911	217	7449	3.1
$A_1 + B_4$		911	216	7446	3.4
$A_1 + B_5$		911	217	7449	3.4
Conventional	$\alpha_1 = 0.6$	1175	122	6830	10.3
$A_1 + B_1 + C_1$		1141	123	6846	2.3
$A_2 + B_1 + C_1$		1158	122	6912	3.9
$A_1 + B_2 + C_2$		1157	125	6928	2.1
$A_1 + B_3 + C_3$		1125	124	6869	1.5
$A_1 + B_4 + C_1$		1143	122	6878	3.1
$A_1 + B_4$		1171	122	6939	3.9
$A_1 + B_5$		1445	139	7459	3.2

Table 5-2: Results of the parameterized MPC approach for different control laws for variable speed limits for $T_c = 5\,\text{min}$. The ramp metering rates are still optimized using conventional MPC. The last column displays the maximum computation time per control time step over the simulation horizon.

the carbon monoxide emissions. So, a trade-off is made between the travel time and the carbon monoxide emissions. This is also visible in the displayed variable speed limits in Figure 5-9, where the maximum allowed speed is almost everywhere below 70km/h over time and space.

The parameterized MPC approach is studied thoroughly, resulting in a lot of simulations of the traffic flow, using the variations of the control laws for different weights of the criteria of the cost function. For each simulation the number of multi-start points n_i, the bounds of θ_i, the choice of the control policy for the parameters of the control laws, and the optimization algorithm have been altered to obtain the best performance compared to the conventional MPC approach, based on trial-and-error. In Appendix B these values are listed per combination of the control laws. However, due to time limitations, the last two combinations of the control laws ($u_{r,o}(k_c+j+1) = D_1 + E_2$ and $u_{r,o}(k_c+j+1) = D_1 + E_3$) have not been tuned extensively.

In Table 5-2 the results of parameterized MPC using different control laws for variable speed limits are listed for two weight factors $\alpha_1 = 1$ and $\alpha_1 = 0.6$. Recall that in these simulations the ramp metering rates are still optimized using conventional MPC. In Table 5-3 the results of the parameterized MPC approach using different control laws for ramp metering rates are listed. In these simulations the control law for variable speed limits $u_{\text{vsl},m,i}(k_c+j+1) = A_1 + B_1 + C_1$ is also included in the parameterized MPC approach.

To get a better overview of the performance of the parameterized MPC approach using the different sets of control laws, in Figure 5-10 the improvement of the criteria is plotted for all the scenarios for $\alpha_1 \in [0.5, 1.0]$, according to Equation 5-7. The value of α_1 is restricted to 0.5, because it was observed in Section 5-3 that lower values did not improve the TTS anymore. Also, to reduce the timespan of the simulations for parameterize MPC for all vari-

$u_{\mathrm{r},o}(k_\mathrm{c}+j+1)$		TTS [veh · h]	TCO [kg]	TFC [l]	Computation time [min]
Uncontrolled		1136	190	7476	0
Conventional	$\alpha_1 = 1$	902	215	7410	17.8
$D_1 + E_1$		935	211	7473	0.4
$D_2 + E_1$		946	202	7395	0.5
$D_1 + E_2$		976	206	7509	0.4
$D_1 + E_3$		924	216	7486	1.2
Conventional	$\alpha_1 = 0.6$	1175	122	6830	10.3
$D_1 + E_1$		1161	122	6929	0.7
$D_2 + E_1$		1168	120	6860	1.3
$D_1 + E_2$		1152	128	6868	1.2
$D_1 + E_3$		1334	122	7089	1.0

Table 5-3: Results of the parameterized MPC approach for different control laws for ramp metering rates, combined with the control law for variable speed limits $u_{\mathrm{vsl},m,i}(k_\mathrm{c}+j+1) = A_1 + B_1 + C_1$ for $T_\mathrm{c} = 5\,\mathrm{min}$. The last column displays the maximum required computation time per control time step over the simulation horizon.

ations of control laws this choice was made.

The performance of the control laws for variable speed limits that uses three parameters in the control laws (the first five variations of the control law) are more or less the same for all the values of α_1. However, when the number of parameters in the control law for variable speed limits is reduced to two, the approach cannot maintain a high performance for all the weights of α_1. The maximum required computation time lies within 3.9 min per control time step. The best control law for variable speed limit is $u_{\mathrm{vsl},m,i}(k_\mathrm{c}+j+1) = A_1 + B_2 + C_2$ with a required computation time of less than 2.1 min per control time step and the best performance.

In Figure 5-10(c) the difference in performance between control laws for ramp metering rates is shown. In this figure it is clearly visible that the performance of the parameterized MPC approach is less than when only the variable speed limits are parameterized. This can partly be explained by the fact that the controller has less degree of freedom to find the optimal control inputs, but also partly due to the fact that the bounds of the parameters θ_i were not selected correctly (see Appendix B). Due to time limitations, the control laws for ramp metering rates have not been studied in detail. Therefore, only for $u_{\mathrm{r},o}(k_\mathrm{c}+j+1) = D_1 + E_1$ and $u_{\mathrm{r},o}(k_\mathrm{c}+j+1) = D_2 + E_1$ the performance is close to the performance of the first five variations of control laws, while $u_{\mathrm{r},o}(k_\mathrm{c}+j+1) = D_1 + E_2$ and $u_{\mathrm{r},o}(k_\mathrm{c}+j+1) = D_1 + E_3$ show poor performance. Note that the maximum computation time of $u_{\mathrm{r},o}(k_\mathrm{c}+j+1) = D_1 + E_1$ and $u_{\mathrm{r},o}(k_\mathrm{c}+j+1) = D_2 + E_1$ combined with the control law of the variable speed limits $u_{\mathrm{vsl},m,i}(k_\mathrm{c}+j+1) = A_1 + B_1 + C_1$ is considerably less than when only the variable speed limits are parameterized. The maximum required computation time lies in the range of 0.4 - 1.3 min. From these two combinations of control laws, the control laws $u_{\mathrm{vsl},m,i}(k_\mathrm{c}+j+1) = A_1 + B_1 + C_1$ and $u_{\mathrm{r},o}(k_\mathrm{c}+j+1) = D_1 + E_1$ is tested to be the best.

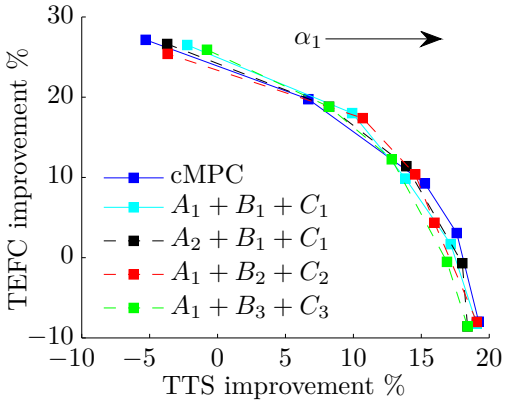

(a) Trade-off curve for different control laws (1)

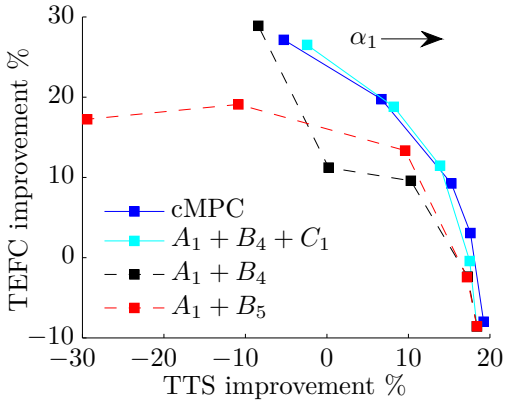

(b) Trade-off curve for different control laws (2)

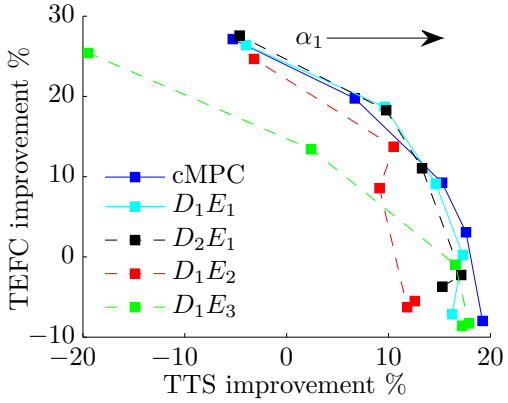

(c) Trade-off curve for different control laws (3)

Figure 5-10: Trade-off curve for different control laws and different weights of α_1. The value of α_1 increases from left to right, starting from 0.5 to 1.0. A lot of control laws show similar performance with respect to the conventional MPC approach.

5-5 Comparison of conventional and parameterized MPC

In Table 5-2, Table 5-3, and Figure 5-10 the parameterized MPC approach is also compared to the conventional MPC approach. From these tables and the figure, it can be observed that the parameterized MPC can maintain a high performance compared to conventional MPC. The first 5 variations of the control law for the variable speed limits (Figure 5-10(a) and 5-10(b)) show a low performance loss compared to conventional MPC. For $\alpha_1 = 1$, the performance loss lies within 1% and for $\alpha_1 = 0.6$ within 5% compared to conventional MPC. The computation time required for parameterized MPC to compute the optimal control inputs is improved from 17.8 min to less than 3.1 min for $\alpha_1 = 1$ and from 10.3 min to less than 3.9 min for $\alpha_1 = 0.6$.

The performance loss for parameterized MPC when both the control measures are parameterized lies within 6% for $\alpha_1 = 1$ and within 2% for $\alpha_1 = 0.6$ for the first two combinations of the control laws. The required computation time reduces even more compared with conventional MPC to less than 1.3 min.

The following conclusions can be drawn from the parameterized MPC results:

1. The studied control laws do not appear to differ much in the performance among themselves, after tuning of the parameters (number of initial multi-start points n_{i}, the choice of the control policy of the parameters of the control laws, and the bounds of the parameters θ_i). Most of the control laws show similar performance for the reduction of the cost function for different weights of α_1. Only four sets of control laws deviate from the trade-off curve of conventional MPC: $A_1 + B_4$, $A_1 + B_5$, $D_1 + E_2$, and $D_1 + E_3$. The performance loss of the first two (i.e. $A_1 + B_4$ and $A_1 + B_5$) can be explained by the fact that the number of parameters in the control law is reduced from three to two with respect to the other control laws for variable speed limits. The control approach does not seem to have enough degree of freedom to compute the optimal control inputs with these control laws. The performance loss of the latter two (i.e. $D_1 + E_2$ and $D_1 + E_3$, in combination with $A_1 + B_1 + C_1$ for variable speed limits) is mainly caused due to the poor selection of the bounds of $theta_0$. Due to time limitations these control laws have not been studied extensively.

2. Since seven of the eleven combinations of control laws have shown good results, it is hard to select the best combination. However, when the assessment of the best control laws is mainly on the reduction of the performance loss compared to conventional MPC and less on the reduction of the computation time, only the control measure variable speed limits should be parameterized, using the control law $u_{\mathrm{vsl},m,i}(k_{\mathrm{c}} + j + 1) = A_1 + B_2 + C_2$ while the ramp metering rates are still optimized using conventional MPC. This results in a performance loss of less than 3% and a computation time of less than 2.1 min per control time step. When the focus lies less on the performance loss compared to conventional MPC and more on the reduction of the computation time, both control measures should be parameterized using the control laws $u_{\mathrm{vsl},m,i}(k_{\mathrm{c}}+j+1) = A_1+B_1+C_1$ and $u_{\mathrm{r},o}(k_{\mathrm{c}} + j + 1) = D_1 + E_1$. This results in a performance loss of less than 6% and a computation time of less than 0.7 min per control time step.

3. The performance loss of parameterized MPC is small compared with the conventional MPC approach (within 6%), whereas the computation time is significantly reduced

(from 10 - 17 min per control time step to 0.4 - 3.9 min per control time step). This enables the use of control laws in the parameterized MPC approach for on-line control of the traffic flow to reduce the travel time, emissions, and fuel consumption.

5-6 Summary

In order to test the MPC approach described in the previous chapters, a case study is conducted. First, a simulation is performed without any control. This results in the formation of congestion at the beginning of the simulation in the vicinity of the second on-ramp, due to the merging of vehicles from that on-ramp to the freeway. The congestion then spills back from the second on-ramp to the origin of the traffic network in a timespan of 40 minutes, after which a queue starts to form at the origin of the traffic network.

With the conventional MPC approach the congestion was resolved only after 5 minutes depending on the weights of the criteria TTS, TCO, and TFC. A balanced trade-off between the criteria is obtained, by adjusting the weights appropriately. For some choice of the weights it is possible to reduce both the travel time and the total emissions and fuel consumption. However, the required computation time of the conventional MPC approach is 2 to 4 times too slow to compute the optimal control inputs.

The results of parameterized MPC show a similar performance (in the range of 1 - 6% performance loss) of the criteria as conventional MPC for different sets of control laws. Moreover, the required computation time is significantly reduced, from 10 - 17 min per control time step with conventional MPC to 0.4 - 3.1 min per control time step with parameterized MPC.

For variable speed limits, the control law can suffice with three parameters to determine the optimal values. When the control law for variable speed limits has only two parameters, the approach fails to maintain a similar performance as conventional MPC. For the control law of ramp metering rates one parameter suffices.

The overall conclusion can be drawn that parameterized MPC is able to yield a similar performance of the reduction of the criteria defined in the cost function as for conventional MPC, however in far less time. In this particular scenario, the computation time limitations of the conventional MPC approach is solved by applying parameterized MPC, so parameterized MPC is shown to be a good alternative for on-line dynamic traffic control.

Chapter 6

Conclusions and future work

6-1 Summary of the thesis

The intensity of vehicles on the road is getting higher each year, resulting in an increase in the occurrence and duration of congestion. The negative impact of congestion is diverse, ranging from extra time spent in the traffic network to an increase in health problems due to the increasing emissions and fuel consumption. Dynamic traffic controllers could be used to reduce the travel time, emissions, and fuel consumption by steering the traffic flows on the traffic network in a desired direction by dynamically adjusting the traffic control inputs, like ramp metering rates or variable speed limits. To compute the optimal control inputs, in this thesis the parameterized Model Predictive Control (MPC) approach is proposed.

Parameterized MPC computes the optimal control inputs based on a prediction of the future traffic states. In this study, two models have been used to simulate the traffic flow (METANET model) and the emissions and fuel consumption of vehicles (VT-Macro model) over a prediction horizon. To determine the optimal control inputs, parameterized MPC relates by some user-defined control laws the control inputs to the traffic states, traffic outputs, and some parameters. The parameters used in the control laws are then optimized via a nonlinear local optimization algorithm in such a way that the objective of the controller is minimized, without violating the constraints active on the system. In this perspective the parameterized MPC differs from conventional MPC, since in conventional MPC the control inputs are optimized directly, without the use of control laws. By applying the control laws, parameterized MPC can reduce the computational complexity of the MPC optimization problem.

The goal of this thesis is to assess the ability of parameterized MPC to reduce the travel time, emissions, and fuel consumption for on-line applications. The controller must be able to compute the optimal control inputs within one control time step, so that it can send these values of the control inputs to the real system. To verify whether the considered approach is able to perform this task, a case study is conducted simulating the Dutch A12 freeway between Bodegraven and Woerden Oost. The parameterized MPC approach is studied for eleven control laws and the performance is compared to the performance of the conventional

MPC approach.

In the uncontrolled scenario congestion occurs in the vicinity of the second on-ramp, due to the high density and the merging behavior of vehicles in the vicinity of the on-ramp. During the simulation, the congestion spills back to the origin of the traffic network and remains unsolved over the simulation horizon of one hour. However, using the parameterized MPC approach the congestion is resolved within ten minutes. Compared to the conventional MPC approach, a similar performance can be realized for most of the sets of control laws (within 6%). In the mean time, the required computation time is reduced significantly, from 10 - 17 min per control time step with conventional MPC to 0.4 - 3.9 min per control time step for parameterized MPC, so since the control time step is 5 min conventional MPC is not feasible in real-time, whereas parameterized MPC is.

The conclusions that can be drawn from the results of the case study are:

- For some values of the weights of TTS (total time spent) and CO emissions in the weighted-sum method the conventional MPC approach is able to reduce both the TTS and the CO emissions at the same time. However, the maximum required computation time is 2 - 3 times too high per control time step, which prevents the use of this approach for on-line applications.
- Seven of the eleven studied variations of control laws of parameterized MPC show similar performance (within 6%) compared to conventional MPC, after fine-tuning of the tuning parameters. However, the reduction of the required computation time is significant, allowing the use of even more complex models. From these seven variations, the control laws $u_{\mathrm{vsl},m,i}(k_\mathrm{c}+j+1) = A_1 + B_1 + C_1$ and $u_{\mathrm{r},o}(k_\mathrm{c}+j+1) = D_1 + E_1$ have been tested the best in performance and computation time.
- Parameterized MPC is able to reduce the travel time, emissions, and fuel consumption for on-line control and is shown to be a good alternative for conventional MPC in this particular scenario.

6-2 Recommendations

The parameterized MPC approach seems to be able to control on-line the variable speed limits and ramp metering rates such that a user-defined cost function is minimized. To this end, a few recommendations are suggested for future research. First of all, the control approach should be validated for other scenarios. Next, to increase the user-friendliness, the use of the ε-constraint method should be investigated. Thirdly, a study can be conducted to see whether or not it is possible to develop a tool that determines the control laws. Finally, other (more complex) applications can be studied using parameterized MPC. These recommendations are elaborated next:

1. *Validation of the control approach.* For the studied scenario, the parameterized MPC approach has shown promising results. However, before this approach can be used in real applications, the performance of the controller needs to be validated for other scenarios as well to guarantee a more general performance assessment of the approach. This can be achieved by altering the demand profile, the case site, or by including disturbances.

Note that the models used in the approach (e.g., METANET and VT-Macro) should be made up-to-date to ensure the accuracy of the control approach.

2. *Study of the feasibility issues of the ϵ-constraint method.* In the case study parameterized MPC aims at the reduction of a multi-criteria cost function, namely the reduction of travel time, emissions, and fuel consumption. The method applied in this project to handle this multi-criteria objective is the weighted-sum method. However, this method does not provide direct insight in the relation between the chosen weights of the criteria and the actual improvement of those criteria. From a user perspective, it is hard to select beforehand the appropriate weights of the criteria that correspond to the requirements of the user. To increase the transparency of the handling of a multi-criteria objective and the actual improvement of the criteria, it is recommended to use the ε-constraint method. This method minimizes one of the criteria, while the other criteria are bounded by some threshold ε. In this method, the user can easily determine the threshold ε, as this resembles the upper bound of the criteria. When the controller is able to find a solution to this problem, it is guaranteed that the constraints are met. In this project, the ε-constraint method resulted in feasibility issues. It is therefore recommended that a study is conducted to find a way to overcome the feasibility issues, so that this method can be used instead of the weighted-sum method.

3. *Study for the development of control laws.* The parameterized MPC approach determines the optimal control inputs by some user-defined control laws. In this thesis, these control laws are based on knowledge of the traffic flow behavior. However, for applications of parameterized MPC where such knowledge is not available, it is hard to design appropriate control laws. Therefore, an alternative approach could be investigated. A study can be performed to develop control laws based on system identification of the available data to estimate the relation of the control inputs and the traffic states and traffic outputs.

4. *Parameterized MPC in other (more complex) applications.* The traffic network considered in this case study is still rather simple. Although the computation time for conventional MPC is already too large for this case study, for parameterized MPC this is not so. Since the number of control variables n_{opt} to be optimized does not depend on the number of control inputs in parameterized MPC, the computation time is also less dependent on the size of the traffic network. It is interesting to research in detail the relation between the computation time (and performance loss) of parameterized MPC on the one hand and the size of the traffic network on the other hand.
   The parameterized MPC approach can also be applied to other more complex applications. In general, whenever conventional MPC is too slow to compute the optimal control inputs, the parameterized MPC framework can be used to reduce the computational complexity of the optimization problem. Such application could for instance be the area-wide reduction of emissions in traffic networks with the control measure route guidance. Thus this also include the dispersion of the emissions to areas near the freeways in the model. This could be interesting e.g., when the production of emissions in a certain area exceeds a safety level. Also other, non-traffic related problems can be addressed with parameterized MPC.

Appendix A

Model parameters

A-1 Parameters of METANET

Table A-1 presents the values of the model parameters used in the simulation to model the traffic flow using the METANET model.

Symbol	Value	Unit	Description
T_s	10	s	Time discretization of the METANET model
i	$1, 2, \cdots N_m$	-	Segment of traffic network
N_m	24	-	Last segment of traffic network
λ_m	3	-	Number of lanes
τ	0.0041	h	Time constant
η_{low}	64.2	km^2/h	Anticipation constant
η_{high}	26.3	km^2/h	Anticipation constant
δ	-0.89	-	Model parameter
κ	32.9	veh/lane/km	Model parameter
κ_v	7	km/h	Model parameter
a_m	2.8	-	Parameter of the fundamental diagram
α	-0.1	-	Non-compliance factor
$Q_{o,1}$	∞	veh/h/lane	Capacity of the road at the origin of the traffic network
$Q_{o,2}$	1750	veh/h/lane	Capacity of the road at the first on-ramp
$Q_{o,3}$	1980	veh/h/lane	Capacity of the road at the second on-ramp
v_{free}	117.7	km/h	Free-flow speed
ρ_{crit}	24.2	veh/lane/km	Critical density of the freeway network
ρ_{max}	187.6	veh/lane/km	Maximum density (or jam density)

Table A-1: Model parameters used in the METANTET model

A-2 Values of the parameter matrix P_y of the VT-Macro model

The regression-based emission and fuel consumption model VT-Macro computes the emissions and fuel consumption factors based on a nonlinear relationship with the space-mean speed and acceleration of vehicles, as defined in Equation 2-22. In this equation P_y is a constant matrix for each type of emission or fuel consumption y and is given by:

$$P_{\mathrm{CO}} = 10^{-2} \begin{bmatrix} 88.7447 & 48.8324 & 32.8837 & -4.7675 \\ 23.2920 & 4.1656 & -3.2843 & 0 \\ -0.8503 & 0.3291 & 0.5700 & -0.0532 \\ 0.0163 & -0.0082 & -0.0118 & 0 \end{bmatrix} \tag{A-1}$$

$$P_{\mathrm{HC}} = 10^{-2} \begin{bmatrix} -72.8040 & 0 & 25.1563 & -0.3284 \\ 8.1857 & 10.9200 & -1.9423 & -1.2745 \\ -0.2260 & -0.3531 & 0.4356 & 0.1258 \\ 0.0069 & 0.0072 & -0.0080 & -0.0021 \end{bmatrix} \tag{A-2}$$

$$P_{\mathrm{NO}_x} = 10^{-2} \begin{bmatrix} -106.7680 & 83.4524 & 9.5433 & -3.3549 \\ 15.2306 & 16.6647 & 10.1565 & -3.7076 \\ -0.1830 & -0.4591 & -0.6836 & 0.0737 \\ 0.0020 & 0.0038 & 0.0091 & -0.0016 \end{bmatrix} \tag{A-3}$$

$$P_{\mathrm{FC}} = 10^{-2} \begin{bmatrix} -67.9940 & 44.3809 & 17.1641 & -4.2024 \\ 9.7326 & 5.1753 & 0.2942 & -0.7068 \\ -0.3014 & -0.0742 & 0.0109 & 0.0116 \\ 0.0053 & 0.0006 & -0.0010 & -0.0006 \end{bmatrix} \tag{A-4}$$

when the inputs of the model are in SI-units and the outputs in kg/s for the emission factors and in l/s for fuel consumption rates [46], [58].

Appendix B

Tuning parameters per control law

In the tables below, the final selection of the tuning parameters n_{i}, the bounds of θ_i, the control policy, and the optimization algorithm, per control law are given.

	n_{i}	$\pm\theta_0$	$\pm\theta_1$	$\pm\theta_2$	control policy	algorithm
$A_1 + B_1 + C_1$	20	1	200	200	variable	active-set
$A_2 + B_1 + C_1$	100	5	50	50	constant	active-set
$A_1 + B_2 + C_2$	5	1	20	20	constant	SQP
$A_1 + B_3 + C_3$	50	5	50	50	constant	active-set
$A_1 + B_4 + C_1$	100	5	50	50	constant	active-set
$A_1 + B_4$	50	5	50	-	constant	SQP
$A_1 + B_5$	150	5	50	-	constant	active-set

Table B-1: List of tuning parameters per control law for variable speed limits. For all scenarios the control time step is equal to 5 minutes.

	n_{i}	$\pm\theta_0$	$\pm\theta_1$	$\pm\theta_2$	$\pm\theta_3$	control policy	
$D_1 + E_1$	10	01	200	200	50	constant	active-set
$D_2 + E_1$	20	01	200	200	100	constant	active-set
$D_1 + E_2$	50	20	200	200	200	variable	active-set
$D_1 + E_3$	50	20	200	200	200	variable	active-set

Table B-2: List of tuning parameters per control law for ramp metering rates. Bounds of the control law for variable speed limit $A_1 + B_1 + C_1$ are also included. For all scenarios the control time step is equal to 5 minutes.

Bibliography

[1] M. Alamir, A. Murilo, R. Amari, P. Tona, R. Fürhapter, and P. Ortner, "On the use of parameterized NMPC in real-time automotive control," in *Automotive Model Predictive Control*, vol. 402 of *Lecture Notes in Control and Information Sciences*, ch. 9, pp. 139–149, Springer, 2010.

[2] A. Alessandri, A. Di Febbraro, A. Ferrara, and E. Punta, "Nonlinear optimization for freeway control using variable speed signaling," *IEEE Transactions on Vehicular Technology*, vol. 48, no. 6, pp. 2042–2051, Nov. 1999.

[3] F. An, M. Barth, J. Norbeck, and M. Ross, "Development of comprehensive modal emissions model: Operating under hot-stabilized conditions," *Journal of the Transportation Research Board*, no. 7, pp. 52–62, Dec. 1997.

[4] C. Audet and J. Dennis, "Analysis of generalized pattern searches," *SIAM Journal on Optimization*, vol. 13, no. 3, pp. 889–903, July 2007.

[5] M. Bell, "Environmental factors in future transport," Tech. Rep., 2006. Foresight Intelligent Infrastructure Systems Project.

[6] T. Bellemans, B. De Schutter, and B. De Moor, "Models for traffic control," *Journal A*, vol. 43, no. 3, pp. 13–22, 2002.

[7] T. Bellemans, B. De Schutter, and B. De Moor, "Model predictive control for ramp metering of motorway traffic: a case study," *Control Engineering Practice*, vol. 14, no. 7, pp. 757–767, July 2006.

[8] E. Camacho and C. Bordons, *Model predictive control*. Advanced Textbooks in Control and Signal Processing, Springer, 2nd ed., 2003.

[9] Centraal Bureau voor de Statistiek, "Indexcijfers van de verkeersintensiteit." http://statline.cbs.nl/StatWeb/publication/?VW=T&DM=SLNL&PA=37674HVV&LA=NL, 2009.

[10] Y. Chiang and J. Juang, "Control of freeway traffic flow in unstable phase by H_∞ theory," *IEEE Transactions on Intelligent Transportation Systems*, vol. 9, no. 2, pp. 193–208, June 2008.

[11] L. Davis, ed., *Handbook of Genetic Algorithms*. New York, USA: Van Nostrand Reinhold, 1991.

[12] H. Dia, S. Panwai, N. Boongrapue, T. Ton, and N. Smith, "Comparative evaluation of power-based environmental emissions models," in *Proceedings of the IEEE Conference on Intelligent Transportation Systems*, (Toronto, Canada), pp. 1251–1256, Sept. 2006.

[13] R. Eglese, "Simulated annealing: a tool for operations research," *European Journal of Operational Research*, vol. 46, no. 3, pp. 271–281, June 1990.

[14] EMFAC 2007, "Calculating emission inventories for vehicles in california," Tech. Rep., 2007. EMFAC 2007 user guide version 2.3.

[15] EPA, "User's guide to MOBILE6.1 and MOBILE6.2: Mobile source emission factor model," Tech. Rep., Environmental Protection Agency, United States, Aug. 2003. Technical Report EPA420-R-03-010.

[16] H. Frey, A. Unal, J. Chen, and S. Li, "Modeling mobile source emissions based upon in-use and second-by-second data: development of conceptual approaches for EPA's new MOVES model," in *Proceedings of Air and Waste Management Association 96th Annual Conference and Exhibition*, (San Diego, CA), June 2003.

[17] C. Garcia, D. Prett, and M. Morari, "Model predictive control: theory and practice - a survey," *Automatica*, vol. 25, no. 3, pp. 335–348, May 1989.

[18] R. Guensler, S. Washington, and W. Bachman, "Overview of the MEASURE modeling framework," in *Transportation Planning and Air Quality III: Emerging Strategies and Working Solutions*, (New York, American Society of Civil Engineers), pp. 51–70, Oct. 1998.

[19] S. Hausberger, R. Pischinger, D. Engler, M. Ivanisin, and M. Rexeis, "Emission functions for heavy duty vehicles," Tech. Rep., Institute for Internal Combustion Engines and Thermodynamics, Graz University of Technology, Vienna, Austria, Feb. 2003.

[20] S. Hausberger, M. Rexeis, M. Zallinger, and R. Luz, "Emission factors from the model PHEM for the HBEFA, version 3," Tech. Rep., Institute for Internal Combustion Engines and Thermodynamics, Graz University of Technology, Vienna, Austria, Dec. 2009.

[21] A. Hegyi, B. De Schutter, H. Hellendoorn, and T. van den Boom, "Optimal coordination of ramp metering and variable speed control - an MPC approach," in *Proceedings of the American Control Conference*, (Anchorage, AK), pp. 3600–3605, May 2002.

[22] A. Hegyi, B. De Schutter, and J. Hellendoorn, "Model predictive control for optimal coordination of ramp metering and variable speed limits," *Transportation Research Part C: Emerging Technologies*, vol. 13, no. 3, pp. 185–209, June 2005.

[23] A. Hegyi, B. De Schutter, and J. Hellendoorn, "Optimal coordination of variable speed limits to suppress shock waves," *IEEE Transactions on Intelligent Transportation Systems*, vol. 6, no. 1, pp. 102–112, Mar 2005.

[24] D. Helbing, "Gas-kinetic derivation of navier-stokes-like traffic equations," *Physical Review E*, vol. 53, no. 3, pp. 2266–2381, Mar. 1996.

[25] S. Hoogendoorn and P. Bovy, "State-of-the-art of vehicular traffic flow modelling," *Proceedings of the Institution of Mechanical Engineers, part I: Journal of Systems and Control Engineering*, vol. 215, no. 4, pp. 283–303, 2001.

[26] Z. Hou, J. Zu, and H. Zhong, "Freeway traffic control using iterative learning control based ramp metering and speed signaling," *IEEE Transactions on Vehicular Technology*, vol. 56, no. 2, pp. 466–477, Mar. 2007.

[27] Z. Huang and X. X. Ma, "Integration of emission and fuel consumption computing with traffic simulation using a distributed framework," in *Proceedings of the 12th International IEEE Conference on Intelligent Transportation Systems*, (St. Louis, Missouri, USA), pp. 154–159, Oct. 2009.

[28] R. Joumard, J. Andre, M. Rapone, and M. Zallinger, "Emission factor modelling and database for light vehicles: Artemis deliverable 3," Tech. Rep., Institut National de Recherche sur les Transport et Leur Securité, Bron, France, June 2007. Report LTE 0523.

[29] M. Kothare, V. Balakrishnan, and M. Morari, "Robust constrained model predictive control using linear matrix inequalities," *Automatica*, vol. 32, no. 10, pp. 1361–1379, Feb. 1996.

[30] A. Kotsialos and M. Papageorgiou, "Motorway network traffic control systems," *European Journal of Operational Research*, vol. 152, no. 2, pp. 321–333, Jan. 2004.

[31] A. Kotsialos and M. Papageorgiou, "Nonlinear optimal control applied to coordinated ramp metering," *IEEE Transactions on Control Systems Technology*, vol. 12, no. 6, pp. 920–933, Nov. 2004.

[32] A. Kotsialos, M. Papageorgiou, C. Diakaki, Y. Pavlis, and F. Middelham, "Traffic flow modelling of large scale motorway networks using the macroscopic model tool METANET," *IEEE Transactions on Intelligent Transportation Systems*, vol. 3, no. 4, pp. 282–292, Dec. 2002.

[33] A. Kotsialos, M. Papageorgiou, and M. M. H. Haj-Salem, "Coordinated and integrated control of motorway networks via nonlinear optimal control," *Transportation Research Part C*, vol. 10, no. 1, pp. 65–84, Feb. 2002.

[34] C. Kouridis, L. Ntziachristos, and Z. Samaras, "COPERT III: Computer program to calculate emissions from road transport," Tech. Rep., Copenhagen, Denmark, Nov. 2000. User manual version 2.1.

[35] P. Li, R. Horowitz, L. Alvarez, J. Frankel, and A. Robertson, "Traffic flow stabilization," in *Proceedings of the American Control Conference*, (Seattle, WA), pp. 144 – 149, June 1995.

[36] Y. Li, B. Waterson, and M. McDonald, "Collection and use of environmental data for transport management: a view from local authorities," *IET Intelligent Transport Systems*, vol. 3, no. 1, pp. 95–101, Mar. 2009.

[37] M. Lighthill and J. Whitham, "On kinematic waves II: A theory of traffic flow on long crowded roads," *Proceedings of the Royal Society A*, vol. 229, no. 1178, pp. 317–345, May 1955.

[38] A. Matzoros, "Results from a model of road traffic air pollution, featuring junction effects and vehicle operating modes," *Traffic Engineering and Control*, vol. 31, no. 1, pp. 24–35, Jan. 1990.

[39] A. Messmer and M. Papageorgiou, "METANET: a macroscopic simulation program for motorway networks," *Traffic Engineering and Control*, vol. 31, no. 9, pp. 466–470, Sept. 1990.

[40] A. Messmer and M. Papageorgiou, "Route diversion control in motorway networks via nonlinear optimization," *IEEE Transactions on Control System Technology*, vol. 3, no. 1, pp. 144–154, Mar. 1995.

[41] E. Negrenti, "The 'corrected average speed' approach in ENEA's TEE model: an innovative solution for the evaluation of the energetic and environmental impacts of urban transport policies," *The Science of the Total Environment*, vol. 235, no. 1-3, pp. 411–413, Sept. 1999.

[42] I. Papamichail and M. Papageorgiou, "Traffic-responsive linked ramp-metering control," *IEEE Transactions on Intelligent Transportation Systems*, vol. 9, no. 1, pp. 111–121, Mar. 2008.

[43] P. Pardalos and M. Resende, *Handbook of Applied Optimization*. Oxford, UK: Oxford University Press, 2002.

[44] H. Payne, "Models of freeway traffic and control," *Simulation Council Proceedings*, vol. 1, no. 1, pp. 51–61, 1971.

[45] L. D. Ragione and G. Meccariello, "Development of an easy module tool based on the kinematic emission model," in *Proceedings of the International Conference on Information Technology Interfaces*, (Cavtat, Croatia), June 2009.

[46] H. Rakha, K. Ahn, and A. Trani, "Comparison of MOBILE5a, MOBILE6, VT-micro, and CMEM models for estimation hot-stabilized light-duty gasoline vehicle emissions," *Canadian Journal of Civil Engineering*, vol. 30, no. 6, pp. 1010–1021, Dec. 2003.

[47] J. Richalet, A. Rault, J. Testud, and J. Papon, "Model predictive heuristic control: applications to industrial processes," *Automatica*, vol. 14, no. 5, pp. 413–428, Sept. 1978.

[48] R. Smit, L. Ntziachristos, and P. Boulter, "Validation of road vehicle and traffic emission models - a review and meta-analysis," *Atmospheric Environment*, vol. 44, no. 25, pp. 2943–2953, Aug. 2010.

[49] R. Smit, M. Poelman, and J. Schrijver, "Improved road traffic emission inventories by adding mean speed," *Atmospheric Environment*, vol. 42, no. 5, pp. 916–926, Feb. 2008.

[50] R. Smit, R. Smokers, and E. Rabe, "A new modelling approach for road traffic emissions: VERSIT+," *Transportation Research Part D*, vol. 12, no. 6, pp. 414–422, Aug. 2007.

[51] H. Teng, L. Yu, and Y. Qi, "Microscale emission models incorporating acceleration and deceleration," *Journal of Transportation Engineering*, vol. 130, no. 3, pp. 348–359, May 2004.

[52] The Mathworks Inc., "Constrained nonlinear optimization." http://www.mathworks.com/help/toolbox/optim/ug/brnoxzl.html, 2011. Last visited on March 07, 2011.

[53] The Mathworks Inc., "Setting options - choosing the algorithm." http://www.mathworks.com/help/toolbox/optim/ug/f12471.html, 2011. Last visited on March 07, 2011.

[54] R. van der Kloor, "Tijdverlies op snelwegen explosief gestegen." http://www.elsevier.nl/web/10194423/Nieuws/Nederland/Tijdverlies-op-snelwegen-explosief-gestegen.htm, June 2008.

[55] S. K. Zegeye, B. De Schutter, J. Hellendoorn, and E. Breunesse, "Model-based traffic control for balanced reduction of fuel consumption, emissions, and travel time," in *Proceedings of the 12th IFAC Symposium on Transportation Systems*, (Redondo Beach, California, USA), pp. 149–154, Sept. 2009.

[56] S. K. Zegeye, B. De Schutter, J. Hellendoorn, and E. Breunesse, "Reduction of travel times and traffic emissions using model predictive control," in *Proceedings of the 2009 American Control Conference*, (Saint Louis, Missouri, USA), pp. 5392–5397, June 2009.

[57] S. K. Zegeye, B. De Schutter, J. Hellendoorn, and E. Breunesse, "Parameterized mpc to reduce dispersion of road traffic emissions." accepted for American Control Conference, June 2011.

[58] S. K. Zegeye, B. De Schutter, J. Hellendoorn, E. Breunesse, and A. Hegyi, "Integrated macroscopic traffic flow, emission, and fuel consumption model for control purposes," *Transport Research Part C*. To appear in 2011.

Glossary

List of symbols

Greek symbols

α	Non-compliance factor
α_i	Weights of criteria in the cost function
β	Turning rate
δ	Model parameter
δ_1	Model parameter for relation CO_2 and fuel consumption
δ_2	Model parameter for relation CO_2 and fuel consumption
η	Anticipation constant
κ	Model parameter
κ_ρ	Model parameter, same as κ
κ_v	Minimum non-zero speed
Λ	Solution boundary
λ_m	Number of lanes of link m
ν	Anticipation constant
ψ	Model parameter
ρ	Traffic density
ρ_{crit}	Critical density
ρ_{max}	Maximum density
τ	Time constant
θ	Parameter used in the control laws
ε	Threshold of criterion in ε-constraint method

Latin symbols

$\hat{x}$	Predicted traffic states
$\hat{y}$	Predicted traffic outputs
a_α	Acceleration of vehicle α

a_m	Parameter of the fundamental diagram of link m
d_o	Demand of traffic network at origin o
$F(\cdot)$	Function of $(\cdot)$ used to map the control inputs
g	Inequality constraints
h	Equality constraints
J	Cost function
k	Time step counter
k_{c}	Control time step counter
l	Time step counter for microscopic models
L_m	Length of each segment of link m
n_{ci}	Number of control inputs
N_{c}	Control horizon
n_{i}	Number of required multi-starts
n_{opt}	Number of parameters to optimize
n_{par}	Number of parameters in the control laws
N_{p}	Prediction horizon
n_{ro}	Number of metered on-ramps
n_{vsl}	Number of independent variable speed limits
N_m	Number of segments of link m
P_y	Model parameter matrix for type y
Q	Capacity of road
q	Traffic flow
q_{cap}	Operational capacity
q_{lim}	Maximum flow
r_{min}	Minimum ramp metering rate
t	Time
T_{c}	Control time step for macroscopic models
T_{m}	Time step of microscopic models
T_{s}	Time step of macroscopic models
u_{ro}	Value of ramp metering rates
u_{vsl}	Value of variable speed limit
v	Traffic speed
$V[\rho]$	Desired or equilibrium speed
v_{free}	Free flow speed
v_{lim}	Speed limit
w_o	Queue length at origin o
CO	Carbon monoxide
FC	Fuel consumption
HC	Hydrocarbon
NO_x	Nitrogen oxide

TEFC	Total emissions and fuel consumption of vehicles in the traffic network
TTS	Total time spent in the traffic network

Subscripts

α	Vehicle of emissions and fuel consumption model
n	Normalization value
off	Off-ramp
on	On-ramp
μ	Link entering node n
σ	Link leaving node n
i	Segment of link m
m	Link of traffic network
n	Node of traffic network
o	Origin of traffic network
y	Type of emissions or fuel consumption

Superscripts

EFC	Emissions and fuel consumption
spat	Spatial-temporal acceleration
temp	Temporal acceleration

Other

$\mathcal{I}$	Set of links entering node
$\mathcal{M}$	Set of links of traffic network
$\mathcal{N}$	Set of nodes of traffic network
$\mathcal{O}$	Set of links leaving node